

Article

Migraine visual aura and cortical spreading depression - linking mathematical models to empirical evidence

Louise O'Hare ^{1,†,*} , Jordi M. Asher ^{2,†}  and Paul B. Hibbard ^{3,†}

¹ Division of Psychology, Nottingham Trent University; louise.o'hare@ntu.ac.uk

² Department of Psychology, University of Essex; jashera@essex.ac.uk

³ Department of Psychology, University of Essex; phibbard@essex.ac.uk

* Correspondence: louise.o'hare@ntu.ac.uk

† These authors contributed equally to this work.

Version May 24, 2021 submitted to Vision

Abstract: This review describes the subjective experience of visual aura in migraine, outlines theoretical models of this phenomenon, and explores how these may be linked to neurochemical, electrophysiological and psychophysical differences in sensory processing that have been reported in migraine with aura. Reaction-diffusion models have been used to model the hallucinations thought to arise from cortical spreading depolarisation and depression in migraine aura. One aim of this review is to make the underlying principles of these models accessible to a general readership. Cortical spreading depolarisation and depression in these models depends on the balance of the diffusion rate between excitation and inhibition, and the occurrence of a large spike in activity to initiate spontaneous pattern formation. We review experimental evidence, including recordings of brain activity made during the aura and attack phase, self-reported triggers of migraine, and psychophysical studies of visual processing in migraine with aura, and how these might relate to mechanisms of excitability that make some people susceptible to aura. Increased cortical excitability, increased neural noise, and fluctuations in oscillatory activity across the migraine cycle are all factors likely to contribute to the occurrence of migraine aura. There remain many outstanding questions relating to the current limitations of both models and experimental evidence. Nevertheless, reaction-diffusion models, by providing an integrative theoretical framework, support the generation of testable experimental hypotheses to guide future research.

Keywords: CSD; non-linear dynamic model; EEG/MEG; fMRI; GABA

1. Introduction

Migraine is a debilitating disorder yet there is little cross-discipline consensus as to its cause. Migraine is heterogeneous, consisting of several subtypes, the most common of which is migraine without aura (MO). However, of interest in the current review are those reporting migraine with aura (MA). These individuals fulfil the International Headache Society diagnostic criteria for migraine, but additionally experience hallucinations around the time of the onset of the headache. The majority of those with MA do not experience the hallucinations on every attack - 79% of those with MA also experience attacks without aura [1]. Migraine aura is thought to be linked to a spreading wave of hyper-excitation (spreading depolarisation) across the brain's surface followed by a period of reduced blood-flow (hypoperfusion) and suppressed neural activity (spreading depression) [2]. It is important to note that the wave of increased activity corresponds to the spreading *depolarisation*, while the suppressed neural activity corresponds to the spreading *depression*. Interestingly, the phenomenology

31 of cortical spreading depolarisation and cortical spreading depression provides an insight into the
32 probable mechanisms underlying migraine aura.

33 This review sets out to match models of migraine aura and the empirical evidence. However,
34 linking the theoretical models of cortical spreading depolarisation and subsequent depression
35 to experimental evidence in humans is challenging. Firstly, it is difficult to obtain direct
36 electrophysiological recordings in humans during an attack due to their fleeting, unpredictable nature.
37 Secondly, in order to model activity directly in humans, extremely invasive procedures would be
38 required in order to capture the activity at the level of cortical columns and ion channels required by
39 the model parameters. It is however possible to extrapolate from animal models to humans, although
40 there are some important limitations that need to be born in mind. For example, along with the
41 differences between human and animal brains, electrophysiological recordings in humans are on a
42 much less fine scale than those obtained from animals. Furthermore, while fMRI techniques record
43 BOLD response, that are indicative of, but not a direct measure of electrical activity in the cortex, it
44 may be possible to relate these to the scale of electrophysiological recordings in humans. Finally, the
45 evidence and knowledge about migraine triggers and behavioural performance may provide some
46 insight into the level of excitation and inhibition in the brain. Although this may be on a different
47 level of abstraction to the level of neurotransmitters, this could still be related to the parameters of
48 model that seek to provide an understanding of migraine aura. While it is currently not possible to
49 draw definitive conclusions, by combining the weight of evidence for what is known about migraine
50 aura phenomenology, triggers and electrophysiological evidence, in this review we seek to draw links
51 between theoretical models of migraine aura and the precise physiological mechanisms to which these
52 models correspond. Effective theoretical models could be used to help combine diverse experimental
53 findings from reported phenomenology, electrophysiology, and behavioural performance, and thus
54 better understand migraine aura. However, the multi-disciplinary nature of the study of migraine
55 means that many models are not accessible to those working in particular domains. The advantage of
56 using these particular models is the flexibility to include abstract elements that mirror the attributes of
57 physical features. These layers of abstraction can, for example be on the level of neurotransmitters or
58 on the level of oscillatory activity related to measured EEG activity. This means that the right level of
59 abstraction can lead to testable hypotheses to better demonstrate the mechanisms in migraine aura.

60 The aims of this review are to (i) provide an accessible introduction to these models and
61 demonstrate how they can test hypotheses related to migraine (ii) to connect how the experimental
62 evidence may support them in the case of migraine and (iii) to highlight the benefits of using these
63 flexible models to obtain insights into the mechanisms of migraine and migraine-aura.

64 1.1. *Phenomenology of hallucinations and visual aura*

65 A hallucination is said to occur when an observer perceives a sensory event in the absence of an
66 external stimulus [3]. Migraine aura is a hallucinatory experience that can occur in any modality. At
67 least 57% of people with migraine aura are thought to experience this visually, [4], and this may be as
68 much as 98% [5].

69 Migraine aura consists of hallucinatory experiences that tend to appear shortly before the onset of
70 the headache itself, the aura symptoms preceding headache onset on average by around 10 minutes
71 [1] (see Figure 1). The duration of the migraine aura is variable, lasting between 5 minutes and 1
72 hour typically [6], the average duration being around half an hour [1]. However, there is also the
73 phenomenon of prolonged migraine aura, which can last over one hour to several days [7]. Hemiplegic
74 migraine aura, which involves weakness of the body, tends to last for longer than one hour [6]. There
75 have been several studies documenting the quality of migraine aura hallucinations, although it must
76 be noted that these vary considerably between individuals [8]. Aura hallucinations are sometimes
77 unilateral, sometimes bilateral; sometimes on the same side as the headache, and sometimes not [8].
78 The most common symptoms of visual migraine aura are the positive symptoms of flashes of light,
79 “foggy” vision, zig-zag lines, flickering lights, and the negative symptom of a scotoma, a temporary

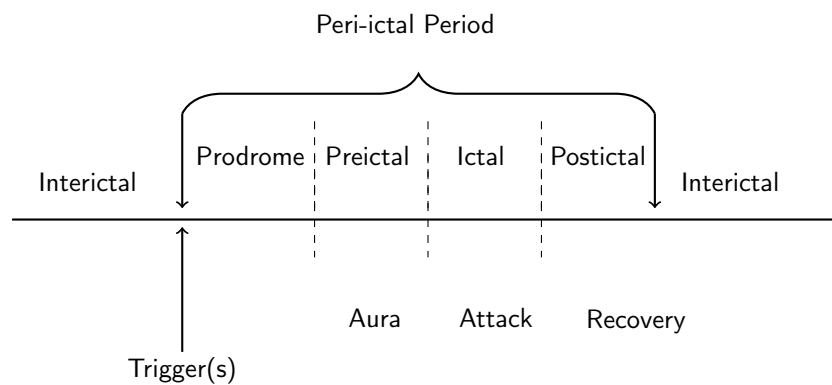


Figure 1. Time course of the stages of migraine

80 blindness in an area of the visual field) [9]. One of the most typical hallucinations is the “teichopsia”, or
 81 “fortification spectrum” which is best described as a “zig-zag” pattern [10]. Illustrations of fortification
 82 spectra have been documented by a range of authors e.g. [11–13] and they are an important tool in
 83 discriminating migraine from other disorders. Finally, while there are also more complex hallucinations
 84 such as the perception of people and objects, these tend to be idiosyncratic and less common than
 85 zig-zags patterns, lines, flashing lights and scintillating scotoma [8,9], and are not considered in the
 86 current review.

87 The individual elements of hallucinations can help discriminate migraine aura from other
 88 disorders, such as the typically reported coloured discs in occipital epilepsy [14,15] or the shorter
 89 duration of hallucinations in visual epilepsy that occur without precipitating triggers [16]. Isolated
 90 attributes of the hallucination alone are not however a reliable means for an accurate differentiation
 91 between migraine and other disorders, which requires that the entire set of hallucinations and the
 92 duration of their effects are taken into account [17], alongside the other defining characteristics of
 93 migraine.

94 The phenomenological qualities of visual hallucinations have been used to generate theoretical
 95 models of the mechanisms of, for example, occipital epilepsy [14,15], Basilar Artery Migraine
 96 (BAM) aura [18], drug-induced hallucinations [19] and hypnagogic hallucinations [20,21]. Thus,
 97 understanding how the specific qualities of the migraine aura correlate with physiological measures in
 98 the brain may give insights into the reasons why these symptoms occur, and thus provide insights into
 99 regarding the nature of migraine itself.

100 The aura can start in either central or peripheral vision [8,22]. One case study reported on an
 101 individual [23] who had recorded their migraine aura for many years. This revealed that their aura
 102 predominantly started in the central visual field, but on occasion started in the periphery. Whilst the
 103 aura was on one side, it could start in either hemifield. Migraine aura is restricted to one or the other
 104 visual hemifield in many people, although it can also be bilateral [8]. fMRI evidence has shown that
 105 migraine aura stops at certain boundaries, corresponding to the sulci [24,25].

106 1.2. Cortical spreading depression as the proposed physiological correlate of aura

107 Cortical spreading depolarisation and subsequent depression is proposed to be the neurobiological
 108 mechanism responsible for migraine aura. Cortical spreading *depolarisation* is characterised by a
 109 massive self-propagating wave of neural activity, informally called a “brain tsunami” [26], which
 110 is followed by a period of suppression of both spontaneous and evoked activity (*depression*) which
 111 propagates over the cortex. The initial wave of depolarisation can be many times the amplitude of
 112 normal spontaneous activity (shown in Figure 2a) and travels slowly at a rate of 2-5mm per minute for
 113 15 seconds or longer [27]. After this initial wave, there is a sustained hyperpolarisation of neurons, and
 114 a reversal of the membrane polarity [28], which inhibits the generation of synaptic potentials. During
 115 this period of silence (suppressed spontaneous activity and reduced excitability), the cortical spreading

116 depression propagates with the depolarisation wave. Recovery can take 5-10 minutes for spontaneous
 117 activity to begin to reemerge [29], but up to an hour [22] to return to normal levels. In contrast, evoked
 118 activity (e.g. as a response from a stimulus) takes longer, around 15 to 30 minutes, to recover [30,31].

119 The spatial and temporal features of the migraine aura have been shown to closely resemble
 120 those of cortical spreading depression [13,29]. The positive and negative hallucinations experienced in
 121 migraine aura are thought to be the result of cortical spreading depolarisation and depression [32],
 122 respectively. Specifically, the zig-zag patterns are thought to be due to the travelling wavefront of
 123 excitatory depolarisation, while the scotoma are thought to be the result of the subsequent depression
 124 of activity [32,33].

125 One of the earliest discoveries of cortical spreading depression was by [Leao](#) [30], who identified a
 126 reduction of the spontaneous activity after applying electrical stimulation to the rabbit, pigeon and
 127 cat cortices [30,34]. However, obtaining electrophysiological recordings for spreading depression in
 128 humans requires subdural electrodes which are usually only used after a traumatic brain injury (e.g.
 129 [35]). Owing to the difficulties and expense in obtaining human data, direct evidence of spreading
 130 depression has not yet been demonstrated during a migraine aura [28,36]. To date non-invasive scalp
 131 based EEG recordings have not captured evidence of spreading depolarisation [34,37], as the spatial
 132 resolution of EEG is not sensitive enough to detect the phenomenon. Evidence of spreading depression
 133 from animal studies has been used to model migraine aura in humans, allowing for closer examination
 134 of the mechanisms of altered cortical and subcortical excitation and inhibition [38]. The most common
 135 elementary hallucinations of migraine aura have been a starting point for mathematical modelling.

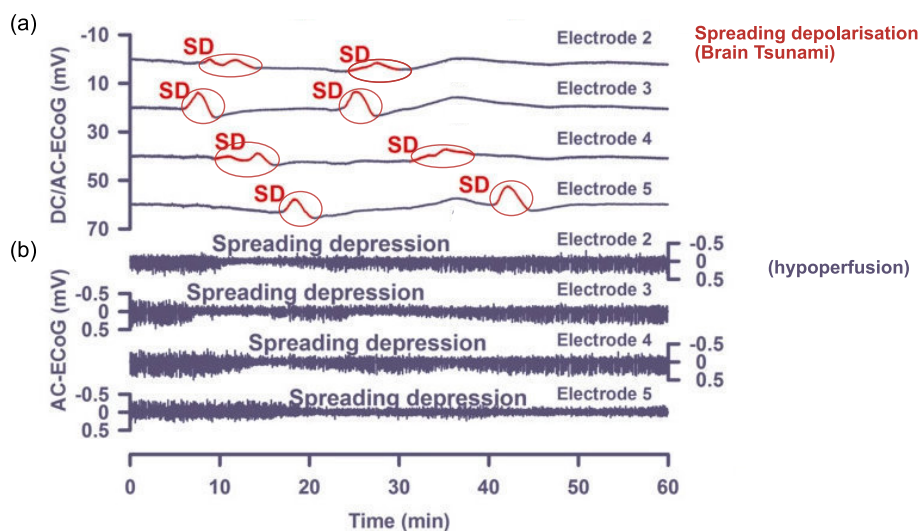


Figure 2. To visualise the electrical activity found in cortical spreading depression we present an excerpt from [Dreier et al. \[27\]](#) (Figure 3: reproduced under the terms of a Creative Commons Attribution Non-Commercial License) of an intracranial recording of spreading depolarisation and spreading depression that was recorded in a terminal patient prior to a stroke. **(a)** DC/AC activity showing the characteristically large depolarisation spreading across a period of an hour **(b)** AC activity illustrating the depression of spontaneous activity caused by the large depolarisation.

136 2. Models of Cortical Spreading Depression

137 There have been several attempts to model cortical spreading depolarisation and the
 138 accompanying hallucinations in general terms (not necessarily specifically for migraine), for a review
 139 see [Billock and Tsou \[39\]](#). It is important to note that many authors use the term "spreading depression"
 140 and "spreading depolarisation" interchangeably (e.g. [40]), as one is considered to follow the other [41].
 141 In animal models reporting recording of the spreading depression, the authors acknowledge that the
 142 silent period follows a wavefront of strong activity [42]. Some authors explicitly acknowledge that

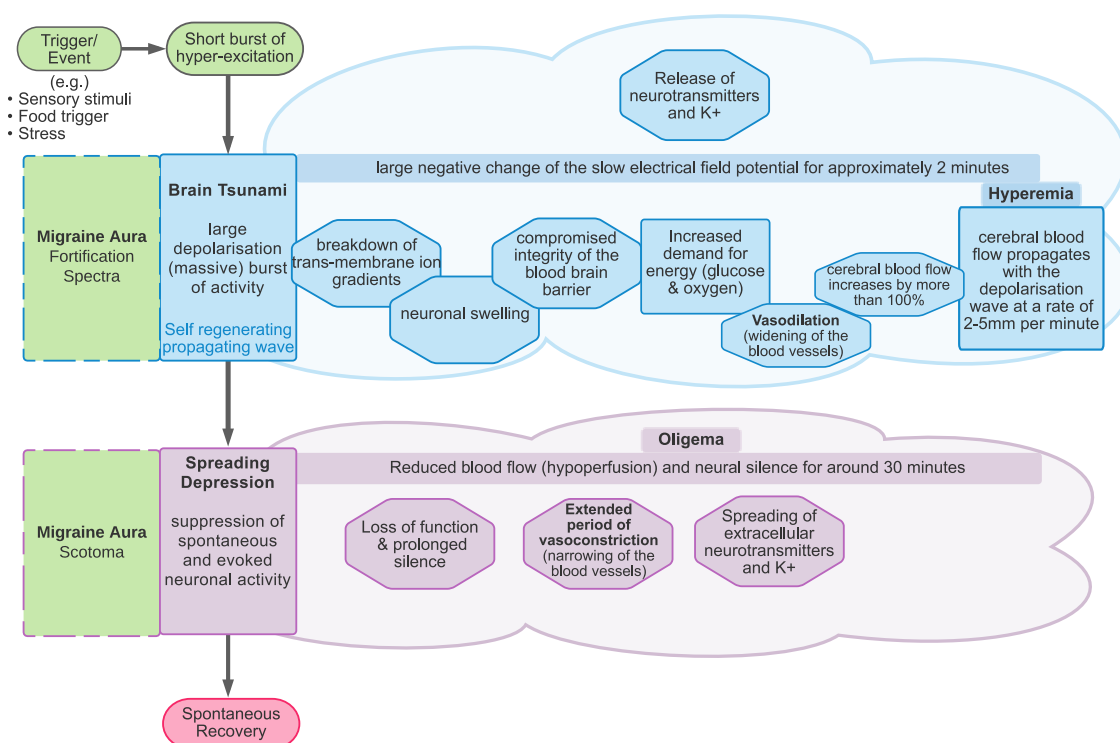


Figure 3. Cortical spreading depolarisation and depression in migraine. Spreading depression and the migraine scotoma start simultaneously with the onset of the negative potential shift of the depolarisation (brain tsunami).

143 the zig-zag patterns and other hallucinations are likely to be the result of the depolarisation wave,
 144 whereas if models are aiming to show the spread of the scotoma then this is likely to be depression that
 145 is of interest [33]. These dynamic models of neural networks are based on reaction-diffusion equations
 146 such as the Wilson-Conwan equation [43,44]. These models capture many of the important properties
 147 of the migraine aura. Firstly, they model both the positive phenomena, such as they appearance of
 148 zig-zag patterns, and the negative phenomenon of the scotoma, as waves of excitation and suppression
 149 respectively. Secondly, they model the propagation of these waves across the visual field. Finally, they
 150 are also able to account for the fine-scale spatial structure of the zig-zag patterns. In this section, we
 151 outline reaction-diffusion models in general terms, and how these have been used as models of cortical
 152 dynamics of the visual brain. We then review their role in explaining the hallucinatory experience of
 153 migraine aura, and the factors that make networks of neurons more susceptible to hallucination in
 154 migraine with aura.

155 2.1. Reaction-diffusion models

156 Introduced by Turing [45], reaction-diffusion models take a theoretical approach to explaining
 157 behaviour and pattern formation [46] in biological, geological and ecological phenomena.

158 For example, one of the more straightforward models, the Gray-Scott equation [47], has been
 159 used to model pattern formation. This example includes two antagonist reagents, A and B, in a
 160 predator-prey-like relationship, modelled by a pair of linked differential equations. Here, two units of
 161 B could for example convert one unit of A into another unit B (the "reaction"), to model B consuming
 162 A. When the levels of A drop, through consumption, then so will the levels of B.

163 In addition to this reaction component of the model, both reagents A and B spread out from areas
 164 of high to low concentration ("diffusion"). Importantly, these diffusion processes occur at their own
 165 independent diffusion gradients, determined by a 2-dimensional Laplacian function. This function
 166 represents the spatial spread of the reagents A and B, from areas of high to low concentration. Examples

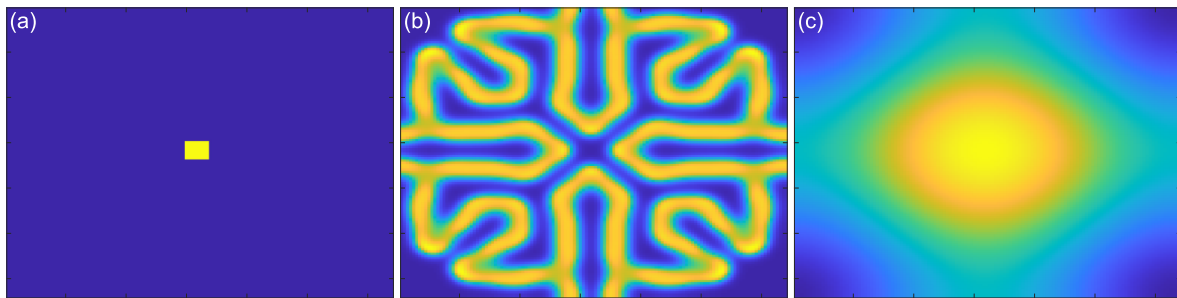


Figure 4. (a) The initial conditions of the activator component of the feed/kill rate model. Most of the area is zero, and there is a central peak seeded at 1, assumed to be due to random fluctuation. (b) The end point of the feed/kill rate model (5000 simulated seconds, with 4 iterations per second). The diffusion rate of the inhibitor (1) is double that of the activator (0.5). (c) The end point of the feed/kill rate model (5000 simulated seconds, with 4 iterations per second), when the diffusion rate of the inhibitor (1) is equal that of the activator (1).

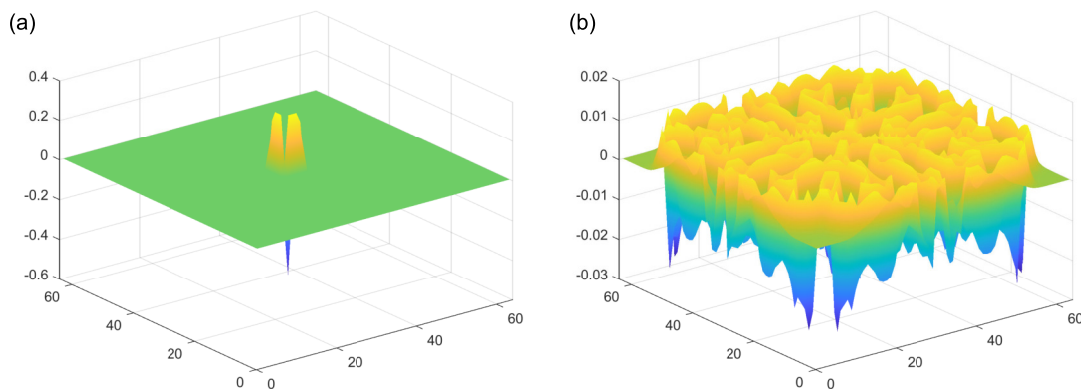


Figure 5. (a) Laplacian function for the initial condition of the activator, showing the direction and rate of the diffusion gradients. (b) Laplacian function for the activator at the end time point, showing the direction and rate of the diffusion gradients.

167 of the Laplacian can be seen in Figure 5. An implementation of this kind of reaction-diffusion model
 168 can be found at: [48]. Critically for the presence of self-emerging patterns, the diffusion rate of the
 169 inhibitor (A in this case) needs to be sufficiently large compared to the activator (B in this case). If this
 170 condition is met, patterns can be formed (Figure 4(b)). By contrast, the output of the model with equal
 171 diffusion rates of the activator and the inhibitor can be seen in Figure 4(c). In this model, there is no
 172 periodic pattern formation. The initial conditions of the activator can be seen in Figure 4(a).

173 Reaction-diffusion models include additional parameters, dependent on the specific model. In the
 174 Grey-Scott model there are additional parameters for a "feed rate" for the introduction of the inhibitor
 175 A into the system, and a "kill rate" for the disappearance of the activator B out of the system. In
 176 the simpler versions of reaction-diffusion equations, these are constants. However, in more complex
 177 reaction-diffusion equations these may be non-linear functions with multiple components. This tends
 178 to be the case in the reaction-diffusion systems representing brain activity, which have been used
 179 to model migraine aura. An excellent explanation is given in the work of [Kondo and Miura \[46\]](#),
 180 summarised here to illustrate how patterns can form and propagate through a network of this type.
 181 The activator increases the levels of *both* the activator as well as the inhibitor in the short-range, while
 182 the inhibitor reduces the level of the activator in the long-range (see Figure 6). Again it is important
 183 that the diffusion rate of the inhibitor B is sufficiently large in comparison to A in order for patterns to
 184 occur. An implementation of a model of this type, based on work by [Gierer and Meinhardt \[49\]](#), can be
 185 seen in Figure 7. In a particular area of the network, there is a random fluctuation resulting in slightly
 186 raised levels of the activator A (Figure 7(a)), which creates a feedback loop further increasing the levels

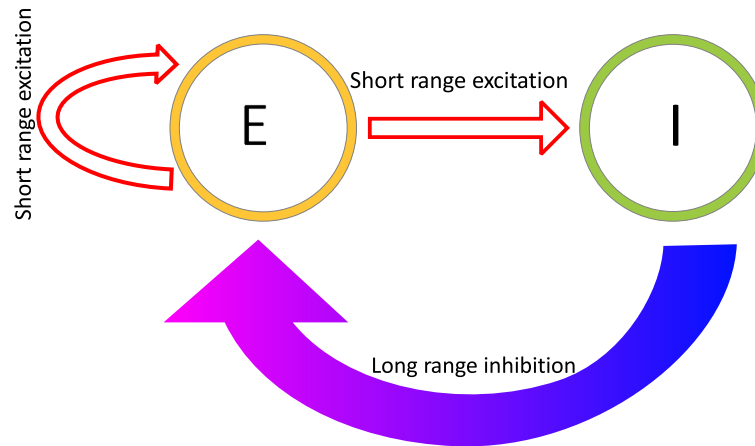


Figure 6. Figure on Activator (E) and Inhibitor (I) reagent levels. The activator E can increase levels of both itself and the inhibitor I, over the short range. The inhibitor reduces the levels of the activator over the long range.

187 of the activation in the area. The levels of the activator thus overshoot the original values. The levels
 188 of the inhibitor increase in response to this activation, Figure 7(b), and reduce elsewhere through a
 189 process of diffusion and decay over time. The shape of the peak of inhibition is slightly lower at the
 190 edges, and the levels of the activator are reduce more in the centre compared to the edges of the area,
 191 resulting in the shape with a dip in the centre compared to the surround Figure 7(c). The activator
 192 enhances its own levels again, as these are higher in the edges this leads to a more pronounced dip in
 193 the centre Figure 7(d). The levels of the inhibitor are also enhanced in the edges compared to the centre.
 194 As the levels of the activator are higher in the centre compared to the surround, this shape is replicated
 195 by the inhibitor, Figure 7(e), creating two peaks in both reagents with a dip in the centre. This relative
 196 release from inhibition in the centre compared to the surround allows the activator to increase again in
 197 the central region, and thus the cycle begins again and periodic patterns begin to form Figure 7(f). The
 198 spatial constraints (Laplacian) and the diffusion rates are key to the pattern formation. If the diffusion
 199 gradients are equal, then the patterns will not occur. Additionally, the model depends on an initial
 200 random fluctuation to begin the self-emerging pattern formation.

201 2.2. Reaction-diffusion models and the brain

202 In the case of the models relevant to the processes of the brain in migraine aura, the activator
 203 and the inhibitor represent the levels of excitation and inhibition at specific locations in a network of
 204 neurons, and the diffusion rates determine the overall speed of propagation of the travelling wave
 205 throughout this network. While these models can be defined on a relatively abstract level, their
 206 components have been linked directly to populations of neurons and their interactions. For example,
 207 [Zhaoping and Li \[50\]](#) has used a reaction-diffusion based model, called the V1 saliency hypothesis,
 208 to replicate human performance on visual search reaction times and performance on figure/ground
 209 segregation tasks. The V1 saliency hypothesis is based on a leaky integrate-and-fire model, a relatively
 210 common model of neuronal spiking. [Zhaoping and Li \[50\]](#) explicitly defines the units as coupled
 211 excitatory pyramidal cells and inhibitory interneurons, and discusses the importance of ensuring that
 212 self-organising patterns of spontaneous activity, giving rise to hallucinatory perceptual experiences,
 213 do not occur.

214 One of the earliest models of the occurrence of hallucinations [\[21\]](#) used a pair of differential
 215 equations to represent excitation and inhibition, as a function of location in the cortex. Excitatory
 216 model units increase activity for both local excitatory and inhibitory units, and inhibitory units can
 217 reduce the activity of local excitatory and inhibitory units. The influence of each unit on the local
 218 activity is represented by a Gaussian weight to represent spatial interactions between cells [\[21\]](#). The
 219 patterns emerge due to the organisation of the network of excitatory and inhibitory units. [Tass](#)

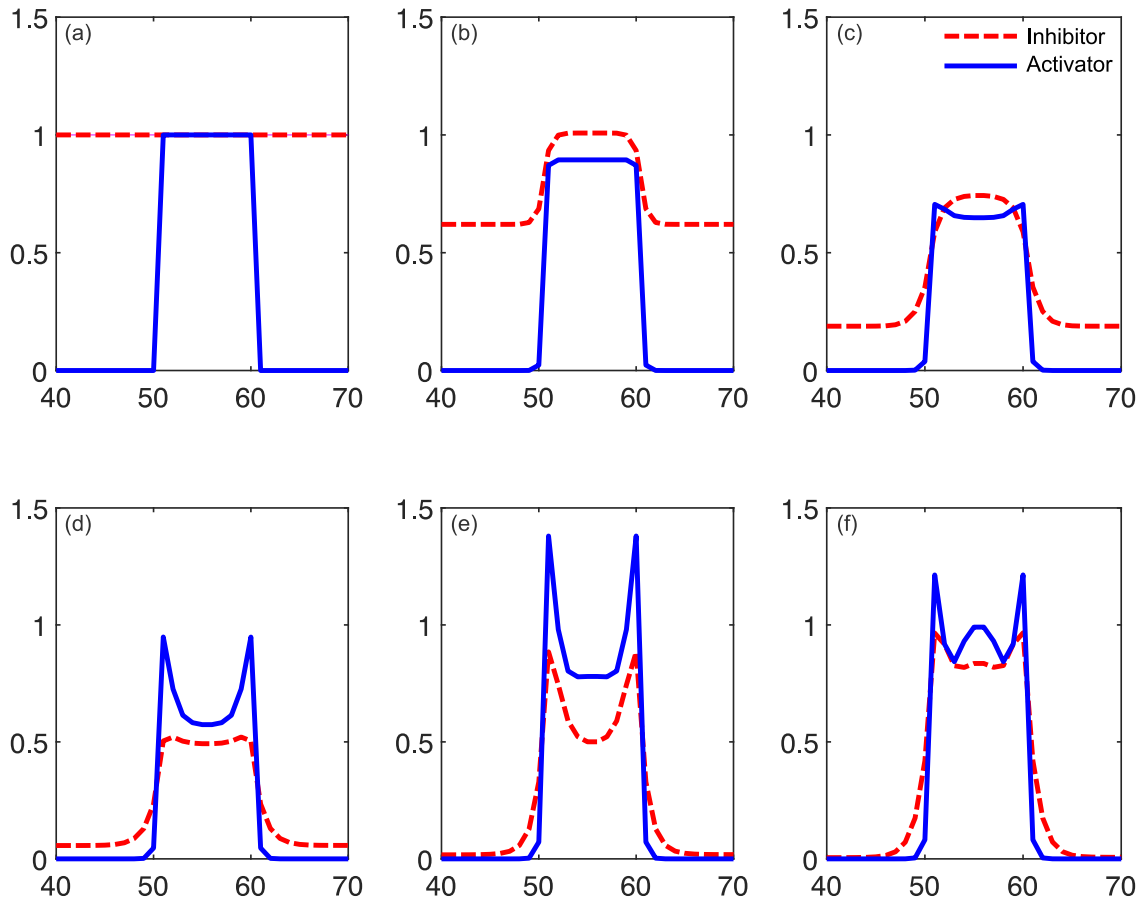


Figure 7. The reaction-diffusion model output for the initial conditions and the first few arbitrary simulated time stages. In this model, the diffusion rate of the inhibitor is twice that of the activator. **a:** shows the initial conditions of the system, the inhibitor is set to 1. The activator is initiated to zero, seeded with an area ("spike") of activity due to random fluctuation. In this spike, the activator is set to 1. **b:** The activator spike has enhanced the inhibitor in that area, and so the inhibitor levels increase to greater than 1 (overshoot) in the region of the activator spike. The inhibitor in other areas has reduced, due to the decay rate. The inhibitor increase is slightly wider than the activator due to the different diffusion rates. **c:** The effects of inhibition can be seen, as the level of the activator reduces. **b:** Inhibitor levels have fallen as there is less of the activator. The activator enhances both itself and the inhibitor, and so at a certain point the levels of activator are low enough that the levels of inhibitor also drop. As the inhibitor has a faster diffusion rate than the activator, this means that the drop is faster for the inhibitor. As the inhibitor has reduced, the activator levels begin to rise again in response to the reduced inhibitor levels - note the edges of the peak, where the reduction in inhibitor is more pronounced and so the increase in activator is beginning to take shape. **e:** the activator levels have risen in response to the reduced inhibitor levels, and this is more pronounced at the edges. Inhibitor levels start to rise again in response. **f:** levels of inhibitor rise again, completing the cycle, this time spatially extended from the original spike location. This continues to create a periodic pattern, under the right conditions.

220 [51] expanded the model to include a control parameter to allow for state switching, for example, to go
221 from below hallucination threshold to hallucinating.

222 These models are based on the physiology of the cortex, and the rate of spread of the hallucinations
223 [39], but they are a general model of hallucinations, not specific to the typical hallucinations of migraine.
224 The earliest models of spreading depolarisation in migraine aura actually modelled the extracellular
225 K⁺ levels (see [40] for a review), which might be considered to be related to cortical excitability. A later
226 model by Reggia and Montgomery [52] included an inhibitor term, and this was able to capture the
227 zig-zag pattern at the spreading depolarisation wavefront.

228 Later work by Dahlem *et al.*, Dahlem and Chronicle [53,54] was aimed at modelling the
229 hallucinations specific to migraine. This model was initially based on the assumption that the cortex
230 is "weakly" excitable, meaning that the excitability levels must be within a certain range relative to
231 threshold to trigger the attack, not much higher (otherwise there will be constant attacks) or much
232 lower, (in which case attacks will never trigger) [55]. This susceptibility term is represented in the
233 non-linear function specifying the reaction rate of the inhibitor, defined in [41].

234 The models aim to replicate the mechanisms of the hallucinations, and they have captured some
235 aspects that relate to the perceptual experience. The models incorporate threshold excitability levels to
236 capture the switching of state of behaviour (bifurcation) from not having an attack to triggering the
237 attack, as in the work introduced by [51]. General models of hallucinations have been able to recreate
238 reported patterns, including spirals and concentric circles [21]. Tass [51] later developed a version
239 able to capture dynamic hallucinations as well (e.g. "blinking rolls") [51]. Terms are also included
240 to represent the propagation boundary conditions, to capture the behaviour of the travelling wave
241 of excitation itself, whether this collapses in on itself or continues through the cortex. In the case
242 of migraine, Dahlem and Hadjikhani [41] successfully replicated the scotoma, and the speed of its
243 propagation over the cortex matched the hallucination expansion.

244 The activity modelled by reaction-diffusion models depends on the excitatory and inhibitory
245 connections between nodes in the network, which depend on their spatial relationship. Since early
246 visual areas in the cortex are retinotopically mapped, there is a strong connection between the relative
247 spatial positions of neurons, and the locations in the visual fields that they represent. There will
248 thus be a similar correspondence between the spatial properties of the reaction-diffusion models,
249 defined by the physical locations of units relative to one another, and spatial position in the image. It
250 is this correspondence that allows the models to capture the spatio-temporal properties of the aura
251 experience.

252 Excitatory and inhibitory connections between units in models of the visual cortex also depend
253 on features beyond the simple location of receptive fields, however. For example, connections that
254 depend on both the location and orientation of features are central to association field models of
255 contour integration [56], and models of visual saliency [50]. This encoding of orientation as well as
256 position is built into the fine-structure of the mapping of properties across the visual cortex, in which
257 clusters of cells encoding similar orientations (orientation columns) form a characteristic 'pinwheel'
258 pattern of variation in preferred orientation [57]. This regular organisation of the primary visual
259 cortex for both position and orientation has been used to provide an explanation of the zig-zag
260 appearance of the aura created by the propagation of the wave of depolarisation Dahlem and Chronicle
261 [54]. This model includes a parameter called the "pinwheel spacing term" to quantify the spacing
262 between orientation columns. By including this fine-scale architecture of the primary visual cortex,
263 and taken into account the orientation tuning of neurons, this model provides a more detailed account
264 of the quality of aura. This is important as it provides a link between the migraine experience, the
265 known dependence of excitatory and inhibitory connections on both location and orientation, and the
266 biological implementation of these functional connections in their spatial mapping in the visual cortex.

267 This model was able to recreate the zig-zag patterns of the fortification spectra at the leading edge
268 of the scotoma, which is a hallucination specific to migraine. They were also able to recreate the reports
269 that migraine aura tends not to engulf the entire cortex, but extends as far as the periphery and then

270 disappears [41]. This is because of the folding of the gyri in the brain. When the brain is convex, the
271 travelling wave will accelerate. When the structure is concave, the travelling wave will decelerate. By
272 considering the folded structure of the human brain, rather than thinking of the space as homogenous
273 or flat, this aspect can be captured effectively.

274 While it may seem unintuitive to link abstract levels and the units of excitatory and inhibitory
275 connections, these models were designed to capture pattern formation in various natural forms. Their
276 strength lies in their ability to abstract the essential components of the network dynamics without
277 needing to know the exact underlying mechanisms [46].

278 2.3. What do models account for

279 Reaction-diffusion based models used to model visual hallucinations are different from simple
280 feedforward convolution-type models of visual processing (e.g. [58,59]), as they do not all rely on an
281 explicit image-forming *stimulus* input in the same way. Rather, they self-generate patterns of activity
282 that correspond to visual hallucinations. The patterns emerge from the initial conditions and the
283 properties of the network parameters, importantly the ratio of diffusion rates between the activator
284 and the inhibitor. This makes them useful in understanding the hallucinations of migraine aura, as in
285 many cases there is no apparent reliable external trigger, but the aura is elicited when certain internal
286 thresholds are reached.

287 The spatial mapping of the models is able to create a travelling wavefront that matches the
288 speed of the progression of hallucinations across the visual field [53]. More recent models [41]
289 have included complex susceptibility terms to recreate both the trigger threshold for the spreading
290 depolarisation and subsequent depression, but also the reason for the hallucination stopping in the
291 periphery. Some models explicitly define lateral interactions (coupling) between units [60], whereas
292 others use Laplacian functions to model these spatial aspects [61]. The Laplacian has been suggested
293 to relate to the connectivity of the brain, which has been able to predict the spatial patterns and the
294 natural frequencies of the oscillatory behaviour [61]. This is a relatively computationally efficient way
295 of being able to model the connectivity for large areas of the brain. Connectivity is something that can
296 be estimated from electrophysiological recordings, which will be discussed later in the review *Section 3*.

297 Reaction-diffusion models have been applied to migraine aura and visual processing more
298 generally in various ways. Some models *do* include a specific input stimulus, which can recreate
299 the oscillatory response and resulting pattern formation from repetitive inputs [60], which may be
300 helpful in relating to neural oscillations measured at the scalp. This will be discussed in more detail
301 in *Section 5*. It is also possible to relate the behaviour of certain reaction-diffusion models to human
302 performance on a visual task [62]. Orientation discrimination performance has been modelled using
303 integrate-and-fire models [63]. Integrate-and-fire models can be considered a simplification of the
304 Hodgkin-Huxley model, which is a model based on a set of reaction-diffusion equations. *Seriès et al.*
305 [63] explicitly defined coupling between units, and defined the spatial distribution using a wavelet
306 function. Orientation tuning sharpening was effectively recreated by this model. The relationship of
307 models to behavioural performance will be discussed in more detail *Section 6*.

308 There are multiple different models of migraine aura, as well as reaction-diffusion models for
309 modelling visual task performance. The difference between those modelling aura and those modelling
310 performance tends to be the input. The former aim to recreate the self-emergent patterns arising from
311 the network properties themselves, the latter focus on accounting for the response of a complex system
312 to a particular stimulus. In order to initiate the self-emerging properties, stochastic (noisy) processes
313 are needed to "seed" the initial reaction. This need not be an external signal, there is the potential for
314 this to be internal to the system. With so many models and variants, it is important to focus on the
315 most relevant ones. *Dahlem and Hadjikhani's* [33] work on recreating the fortification patterns specific
316 to migraine is an important step here. This group has successfully developed models recreating many
317 of the aspects of migraine aura, by including appropriate parameters. The next issue is what the

318 parameters represent in terms of biological systems in the brain itself. Several suggestions have been
319 made, and this will be covered in the next section.

320 3. Linking models to physiological differences in migraine

321 The models use terms defining excitation and inhibition, but in order to transition from the
322 abstract model these terms must have some physiological basis. Mechanical and electrical stimulation
323 of the cortex can induce spreading depression in animal models, as can chemical methods such as
324 introducing KCl and GABA [2], suggesting that the answer may be a complex interplay of several
325 factors.

326 3.1. Ion transfer

327 One suggestion is that these terms relate to the transfer of ions across the cell membrane. For
328 example, the models of Dahlem et al., [53,54] suggest that their excitation term could represent the
329 level of extracellular potassium ions (K⁺). Changes in the levels of extracellular K⁺ (both increase
330 and decrease) have been shown to increase the chances of spreading depression in the chicken retina
331 [64]. Sleep deprivation, a commonly reported migraine trigger (e.g. [65]), increases the extracellular
332 K⁺ levels in animal models, and also lowers the spreading depression threshold [66]. Additionally,
333 changing from stationary to locomotion increases K⁺ levels [67], and physical activity can aggravate
334 migraine [68].

335 Increased spike activity increases extracellular K⁺ [69]. Smith *et al.* [2] suggested the rapid increase
336 in K⁺ following intense neural firing results in the propagation of spreading depression, and that this
337 might be controlled by NMDA [2]. Astrocytes seem to be key in protecting against the onset of the
338 travelling wave [2,31], and these cells have an important role in K⁺ homeostasis [70]. Astrocyte density
339 is lower in the visual areas of the brain, which might explain why spreading depression is relatively
340 easy to trigger here [31]. However, K⁺ is not released before the onset of depolarisation of the cells,
341 and glutamate release follows the K⁺ release, suggesting that these changes may be secondary to the
342 onset of the attack [71].

343 K⁺ increase is only one aspect of the complex ion changes in spreading depolarisation and
344 depression. As well as the increase in K⁺, the levels of Cl⁻, Ca²⁺ and Na⁺ all decrease [72]. However,
345 the K⁺ is of particular interest as this seems to be the key ion involved in CSD development - when
346 the K⁺ threshold is reached, this initiates the CSD. Additionally, this can be prevented if the glial cells
347 (which control K⁺ levels) are able to act [72].

348 A study involving introducing a pathological mutation (knock-in) into mice resulted in increased
349 susceptibility to CSD, and this mutation specifically affected the Ca²⁺ channels [73]. As the Ca²⁺
350 channels have a role in controlling neurotransmitter release, particularly glutamate [74], this may be
351 the mechanism of the CSD. Additionally, these channels also have an indirect role in the release of the
352 neurotransmitter GABA [75].

353 Estimating the involvement of specific ions is difficult as the change in concentration in other ions
354 cannot be easily controlled in investigations of the spreading depression. For example, animal models
355 show changes in Cl⁻ concentration (an increase after an initial decrease) after repetitive stimulation
356 in cat sensorimotor cortex [76]. It has been suggested that the ion transfer of the different ions are
357 dependent on each other, for example as K⁺ leaves the cells, Na⁺ ions exchange places, although the
358 exchange with Na⁺ is not 1:1 [77]. Additionally, there is the issue of electrodiffusion [40]. As the ions are
359 electrically charged, this will counteract any diffusion gradient unless the other (negatively) charged
360 ions also move. Taken together, this makes it very difficult to isolate the ion of interest experimentally,
361 and so although the most likely candidate seems to be K⁺, this is far from conclusive.

362 3.2. GABA

363 Neurotransmitters such as gamma-aminobutyric acid (GABA) could also be involved in the level
364 of inhibition. Dahlem and Chronicle [54] suggest that GABA might be deficient in the cortex of those

365 with migraine, and that extracellular K⁺ is the triggering factor for the attack itself. Increasing the level
366 of GABA results in increased extracellular K⁺ [78]. However, a review of epilepsy suggests that GABA
367 seems to affect Cl⁻, rather than extracellular K⁺ [79].

368 Using the GABA antagonist Metrazol, which disturbs the action of GABA, to activate the cortex
369 in conjunction with 8-10Hz photic stimulation resulted in spreading depression [80]. Those with MA
370 taking a GABA agonist (sodium valporate) showed normalised performance on a psychophysical task
371 (metaccontrast masking) compared to those not taking this medication [81]. Sodium valporate also
372 normalises transcranial magnetic stimulation (TMS) phosphene excitability [82]. Importantly, there are
373 links between behavioural performance and GABA levels - in healthy participants, increased GABA
374 levels relate to increased orientation discrimination specificity [83]. A more detailed discussion of
375 behavioural tasks thought to rely on GABA concentration in those with migraine specifically will be
376 discussed in *Section 6* below. Spreading depolarisation can be aborted in human cortex (in vitro) with
377 the introduction of GABA [84].

378 In humans, some authors report that GABA concentration does not differ between migraine and
379 control groups, or between those with MA and MO [85,86]. However, others have shown lower levels
380 of GABA, specifically in those with MA compared to controls [87]. It must be noted that these studies
381 tend to have a relatively limited sample size due to the expensive methodology. Additionally, other
382 authors reported increased GABA was related to increased pain and severity [88], which does not
383 support the idea that a lack of GABA is the problem in those with migraine. GABA agonists have
384 shown some benefit in migraine e.g. [89], for a review see [90]. However, according to a Cochrane
385 Review, gabapentin, which increases GABA levels in the brain [91], does not help much for migraine
386 prophylaxis [92].

387 3.3. *Glutamate*

388 Glutamate is another neurotransmitter related to migraine pathophysiology. Interictal glutamate
389 levels in occipital cortex have been shown to be higher in a mixed group of migraine with and without
390 aura compared to controls [93]. Many studies estimate levels of combined glutamate and glutamine
391 (Glx), and this combined measure is also higher in migraine compared to controls [94]. Interictal MA
392 showed higher levels of glutamate compared to controls, but glutamate levels did not correlate with
393 VEP responses [95]. Findings on this are mixed, as other authors have shown no overall differences in
394 glutamate levels, but a relationship between BOLD activity in response to chequerboard stimulation in
395 those with MA [87]. It could be the case that specifically MA, and specifically in the occipital areas,
396 there are differences. Studies of this kind tend to have relatively small sample sizes due to their
397 expensive nature and so this decreases the reliability of statistical findings. A recent study showed that
398 glutamate and GABA levels can correspond to occipital activation, but this depends on the current
399 state - GABA correlated with brain activity under dark conditions, whereas glutamate levels correlated
400 with the brain's responses to chequerboard stimulation [83]. This study could help understand the
401 mixed findings in previous research into glutamate and GABA in migraine - findings are likely to
402 depend on the state of the visual brain at the time, whether processing information or resting. Many
403 studies into the role of glutamate actually estimate the Glx combined measure. Glx contains both
404 glutamate and glutamine. Glutamine is the precursor to both glutamate and GABA [96], and so results
405 must be interpreted with caution, as it is possible that there is a simultaneous increase in GABA levels
406 due to the glutamine.

407 3.4. *Electrical stimulation*

408 Direct electrical stimulation of the cortex has been shown to elicit spreading depression in animal
409 models [30]. Intracranial strip recordings of migraine aura over the frontal areas have shown evidence
410 of spreading depression, including a sharp increase in activity, followed by a "DC shift". The DC
411 shift indicates a reduction in activity compared to spontaneous levels of activity before the aura event
412 [71]. A less invasive method of stimulating the cortex in human observers is to use transcranial

413 direct current stimulation (tDCS), transcranial alternating current stimulation (tACS), or transcranial
414 magnetic stimulation (TMS). Electrical stimulation (tACS) of the cortex can elicit phosphenes[97], but
415 these do not tend to resemble the fortification spectra commonly reported in migraine [39].

416 3.5. *Links between models and biology*

417 Linking the model parameters to biological systems in the brain is not a straightforward
418 process. There are several suggestions for what the parameters in the models might represent,
419 outlined schematically in Figure 8. At this stage, it seems that there is no agreed answer, due to
420 the complexity of both the models and the neural system, the expense of experimentally estimating
421 levels of neurotransmitters, and most importantly the substantial variation between individuals with
422 migraine. In order to gain some insights, large-scale longitudinal studies may be needed. Whilst these
423 may pose logistical and expense issues for methods such as spectroscopy, there may be behavioural
424 possibilities to investigate these differences. For example, [Smith et al. \[98\]](#) showed (indirectly) that it
425 may be possible to increase levels of GABA through diet, demonstrating an effect on EEG responses
426 over several sessions, and an appropriate washout period. Using spectroscopy might be the gold
427 standard for measuring neurotransmitter levels, but the cost of longitudinal studies of larger groups
428 (to allow for individual variation) may make this prohibitively expensive. However, it may be possible
429 to supplement these studies using behavioural techniques such as [Smith et al. \[98\]](#). Additionally, the
430 triggers of migraine could also give some insights into the system before the onset of the migraine
431 attack.

432 4. Linking models to known migraine triggers

433 The factors that can precipitate a migraine attack may be particularly useful for understanding
434 the onset of the attack and the migraine aura. A survey of 181 individuals with migraine reported that
435 common triggers are stress, light, emotions, sleep disturbances or alcohol useage [65]. A systematic
436 review of migraine triggers, based on self-report in most studies, found the most commonly reported
437 triggers to be stress (58% migraineurs), auditory stimuli (56%), fatigue (43%) fasting (44%), hormonal
438 factors (females only, 44%), sleep disturbances (43%), changes in weather (39%), visual (38%) and
439 olfactory (38%) factors and alcohol (27%) [99]. Stress was also the most commonly reported trigger in
440 several other studies [100–103].

441 4.1. *Food based triggers*

442 Food is also commonly reported as a trigger for migraine, for example, red wine has been
443 listed as a migraine trigger [103]. Red wine has anti-seizure effects by inhibiting firing rate through
444 closing Na⁺ channels and opening Ca²⁺ channels [104], which would be thought to protect against
445 spreading depolarisation and depression. However, given the complex interplay between ions and
446 neurotransmitters, this may be an oversimplification of a complex system. Chocolate has also been
447 reported as a trigger [103], by around 19% of participants [105], however, studies trying to elicit
448 migraine attacks using chocolate have failed [106]. Moreover, serotonin and magnesium are relatively
449 high in chocolate, and these are thought to prevent migraine attacks [106]. Chocolate affects brain
450 oscillations, increasing alpha and beta, and decreasing theta and delta activity [107]. Garlic oil has
451 been shown to reduce the amplitude of KCl triggered spreading depression in rats, and this is possibly
452 due to an effect on astrocytes [108].

453 There have been questions about the reliability of self-reported triggers - only a few people (3/27)
454 could precipitate a migraine attack from their self-reported triggers [109]. It may be the case that
455 reported triggers are not causal, merely correlated with the migraine attack. Theoretically, it may be
456 more useful to look at triggers that can induce migraine more reliably, however, there are obvious
457 difficulties with this approach. Visual triggers have however been successfully demonstrated to be
458 capable of inducing migraine [110].

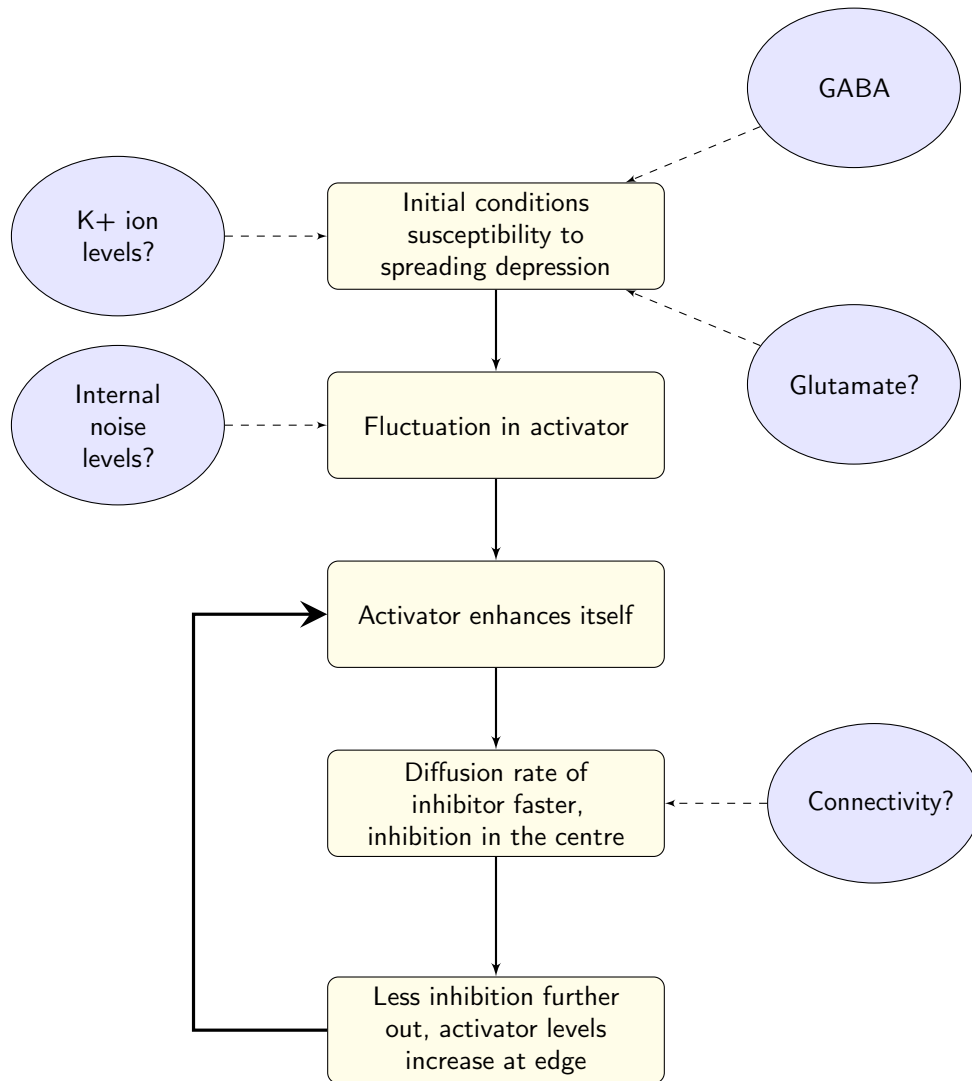


Figure 8. A schematic diagram of the main model stages and the possible parameters that have been associated with spreading depression. The initial conditions (prior to the initiating event) represent the susceptibility of the cortex to spreading depolarisation and subsequent depression. This could be due to neurotransmitters such as GABA, glutamate, and K^+ ion levels. The next stage is the precipitating event, represented in the model by random fluctuation in activity. It is possible that random fluctuation is more likely in those with migraine due to increased internal noise in the brain. The next stage of the model is the self-enhancement of the activator. One of the key points for pattern formation is the ratio of diffusion rates for the activator and the inhibitor, which feasibly relate to the coupling strength or connectivity within the brain.

459 4.2. Sensory triggers

460 Sensory triggers may be more specific to migraine compared to other headache disorders. Stress
461 and lack of sleep were triggers common to both migraine and tension-type headache, whereas sensory
462 factors such as weather, smell, smoke and light differentiated between migraine and tension-type
463 headache [102]. Similarly, both control and migraine groups commonly reported stress and tiredness
464 as headache triggers, however 45% of those with migraine, and only 6% of controls, reported visual
465 triggers [103]. Visual stimuli included flickering lights, striped patterns, and also computer screen
466 use, reading, bright colours and optic flow stimuli. Interestingly, light was reported as a trigger in a
467 relatively high percentage of the younger individuals with migraine (10-19 years) [111].

468 Flicker has been shown to elicit headache in both migraine and control groups, although those
469 with migraine reported experiencing more severe symptoms. This study used 5Hz stimulation for 5,
470 10, 15, 25 and 35 minutes, with 15 and 25 minutes of stimulation leading to the most intense headaches.
471 As the longest period of stimulation did not lead to the most intense headaches, the author suggests
472 this may indicate habituation to the stimuli [112].

473 4.3. Modelling triggers

474 Migraine triggers vary widely, seem to be idiosyncratic and are unreliable, making it difficult to
475 link triggers to models directly. However, there are some more common triggers, such as stress and
476 sleep deprivation, which may give insights into the state of the brain, e.g. in terms of K⁺ levels. It
477 seems that in general sensory stimulation is more specific to those with migraine compared to other
478 types of headache, although this is not a rule. Repetitive light stimulation has been shown to have
479 an effect on glutamine levels in those with migraine - baseline levels were elevated in those with
480 migraine compared to controls and reduced with repetitive photic stimulation in those with migraine
481 only [95]. Lowered glutamine levels might be expected to *decrease* excitability, as they are the precursor
482 to glutamate, and so this seems counter-intuitive that there would be a reduction in excitability to
483 precipitate an attack. However, as previously mentioned, glutamine can also be the precursor for
484 GABA [96], and so the effects of photic stimulation may not only affect excitation, but also inhibition
485 levels.

486 In addition to changes in neurotransmitter levels, oscillatory neural responses are affected by
487 repetitive visual stimulation [113]. This can be a link to both the models, which have been used to
488 represent oscillatory brain activity, and to brain activity during migraine aura. Due to the spontaneous
489 and fleeting nature of the attack, recordings during the aura phase are relatively rare, however, some
490 have been achieved and the evidence will be discussed in the next section.

491 5. Linking models to neural activity during aura (and headache)

492 In order to link theoretical models to migraine in human observers, it would be useful to use
493 recordings of brain activity, such as electroencephalography (EEG) and fMRI. There are reports of EEG
494 differences in migraine between attacks (interictally), although this is not sufficient for use as a
495 diagnostic tool [14]. Abnormal interictal EEG is more likely in those with aura compared to those
496 without, and the most common abnormalities were slow waves and spike activity [114]. A review
497 of the interictal literature in EEG in migraine reported that the most commonly reported findings
498 include increased slow wave, theta, and delta power, although the literature is rather mixed [115].
499 Some authors found reduced alpha frequency between migraine and control participants [116,117].
500 Differences in alpha power have been reported to be related to migraine history (those with the longest
501 history of migraine, approximately 5 years in a paediatric sample) [118], and also to fluctuate with
502 proximity to the attack [119]. There have in addition been reports of asymmetry of alpha power
503 between the hemispheres [120] [121]. There are also reports of interictal increases in power in beta
504 band (12-20Hz) oscillations [117]. Interictal EEG shows increased theta band power compared to
505 controls in a group including both MA and MO participants [122].

506 Repeated testing at several points during the migraine cycle has been conducted using
507 electrophysiological methods also. [Sand et al. \[123\]](#) reported increased P1N2 amplitude before attack in
508 a mixed migraine group, and [Sand et al. \[124\]](#) reported increased N1P1 and P1N2 responses specifically
509 in those with migraine aura, which increased before the attack compared to interictally. [Shibata
510 et al. \[125\]](#) reported increased N1P1 amplitude in MA shortly after the attack. Studies investigating
511 habituation of VEP responses found reduced habituation in migraine interictally, but this seems to
512 normalise by increasing to more control-like levels immediately before the attack [126,127]. Evidence
513 has shown that a measure called the "Brain Engagement Index" correlates with the proximity to
514 the migraine attack, peaking before the attack (preictal stage) and reducing afterwards. The Brain
515 Engagement Index was identified as the frequency of occurrence of an individual-specific template
516 of ERP activity in the delta band (1-4Hz) [128]. This is important as delta band suppression is the
517 EEG correlate of depolarisations measured using intercranial recordings in those with traumatic brain
518 injury [35].

519 In order to understand the aura itself, and to link to models of spreading depolarisation and
520 depression, recordings are needed during the attack phase (ictal recordings). There are difficulties in
521 recording brain activity during migraine attacks, due to their unpredictable, and short-lived nature.
522 However, some recordings have been made, generally either recording those with very frequent or
523 chronic attacks, or by inducing an attack.

524 5.1. Slow waves

525 One of the earliest studies into EEG in those with migraine studied 51 participants in varying
526 phases of the attack - interictal (between attacks) in some, but also some recordings were made during
527 the aura phase. One such study recorded from individuals with basilar-type migraine (BAM), a
528 less common variant of migraine with aura [129]. BAM originates in the brainstem of both occipital
529 lobes, and is commonly accompanied with vertigo and lack of co-ordination [130]. 30 of the 51 were
530 shown to have "abnormal EEG", although the record lacks details on the abnormalities. Slow wave
531 (5-8Hz) abnormalities were reported, and these were exaggerated during the aura in some individuals.
532 However, in other individuals there were normal resting states and no change in EEG activity reported
533 during the migraine attack phases. Activity seems to be lowered during the main headache stage [129].

534 Other researchers have also reported pronounced slow wave activity during an attack in the
535 posterior areas of the brain in those with BAM [131], specifically in the theta band [132]. [Soriani
536 et al. \[133\]](#) reported "diffuse and continuous" reduced alpha, but increased beta band activity, as well
537 as posterior slow waves. After the onset of the headache, there has been increased activity in the
538 delta/theta bands in children with migraine, and no abnormalities were found interictally [134]. Other
539 researchers have reported the band to be lower still, diffuse slow activity in the delta-subdelta range
540 (0.5-2Hz) in children 4 hours after the onset of the attack [135]. All of the participants had normal or
541 improved EEG 4 days after the attack, again suggesting the EEG normalises interictally. In the case of
542 one paediatric participant who experienced migraine aura without headache, EEG recording made the
543 day after the attack showed there to be left occipital slow waves. Additionally, magnetic resonance
544 (MR) perfusion showed hyperperfusion (increased blood flow) over parietal-occipital areas. These
545 changes returned to normal 3 days after the attack [136].

546 Hyperventilation has been used to elicit migraine attacks, and has resulted in changes to theta
547 and delta band activity; specifically, the delta band changes were bisynchronous slow waves (2-3Hz)
548 recorded over frontal electrodes [137]. The authors did not include details of the photic stimulation
549 used and so it is unclear why this would not have affected the EEG recording [137]. A PET scan of a
550 spontaneous migraine aura showed there to be spreading hypoperfusion (reduction in blood flow)
551 with time [138]. Migraine aura has also been induced by injection of Xenon (Xe) in the carotid artery.
552 This was successful in 9 out of 13 participants in a study by [Lauritzen et al. \[139\]](#). Low blood flow
553 was demonstrated on the same side as the injection, starting in posterior areas and spreading through
554 the cortex. However, this low blood flow did not cross the sulcus [139], an attribute of migraine aura

555 that has been modelled successfully as being due to the gyrification of the cortex [64]. Participants
556 who experienced an attack after the Xe injection showed hypoperfusion in posterior areas of the brain,
557 including the occipital, posterior parietal, and posterior temporal areas. Interestingly, rCBF remained
558 unchanged in those who did not experience an attack after the injection [140]. Hypoxia has been used
559 to trigger migraine attacks [141], and hypoxia results in K⁺ and is related to the spreading depression
560 in animal models [142]. This indirectly links excitability, spreading depolarisation and depression, as
561 well as electrophysiological activity.

562 Lee *et al.* [143] reported several EEG recordings in a case study of hemiplegic migraine (which
563 included confusion and motor aphasia). Hyperventilation and photic stimulation did not affect EEG
564 in this patient, unusual EEG activity "diffuse slowing" was seen after sleep deprivation. During the
565 recording of sleep activity, POST (positive occipital sharp transients) were seen. A large review of EEG
566 studies reporting POSTs found these to be more common in younger individuals, and more likely to
567 be accompanied by EEG abnormalities (including slowing and epileptiform activity), compared to
568 controls [144]. Future work investigating POSTs and activity after sleep deprivation may be particularly
569 useful in understanding migraine, however, there are too few controlled sleep trials involving those
570 with migraine to form any conclusions on this at present.

571 Other authors have reported changes to electrophysiological activity during recordings of
572 visually-induced migraine aura. Bowyer *et al.* [110] recorded MEG during the migraine aura either
573 from spontaneous (4 individuals) or induced (8 individuals) attacks. The attack was induced using
574 black and white chequers reversing at 8Hz. Those with spontaneous aura showed activation in the
575 right occipital-temporal/parietal region. Those with induced aura showed activation in the primary
576 visual cortex, left occipital and right temporal areas. Direct current (DC) shifts were taken as a measure
577 of activation, and DC shifts were only seen in those with migraine, not in the control group. DC shifts
578 are an overall increase in the amplitude of the measured response, and can be indicative of 0.1 to
579 0.2Hz slow potentials [145]. These DC shifts were suggested to be indicative of extracellular potassium
580 accumulation and the accompanying spreading depolarisation and subsequent depression [110]. In
581 the cat, negative DC shift is related to membrane depolarisation, which is linked to pyramidal cell
582 activity [146]. This is important as pyramidal cells have been suggested to be a possible biological
583 implementation of the excitatory component of reaction-diffusion models e.g. [50].

584 5.2. Beta band oscillations

585 Kanai *et al.* [97] showed that electrical brain stimulation in the beta range (14-22Hz) makes it easier
586 to elicit flickering phosphenes. How readily phosphenes are elicited is generally considered a measure
587 of cortical excitability [147,148]. During the interictal period, after 30 seconds photic stimulation at
588 frequencies of 2, 4, and 6Hz, the beta band amplitude (recorded over temporal areas from channels
589 T3-T5) of those with migraine was found to be increased compared to controls, whereas in those
590 with epilepsy the alpha band amplitude increased with flash stimulation. Unlike epilepsy, those with
591 migraine showed no differences in the power spectral density (PSD) in the absence of flash stimulation
592 [149], showing that the visual stimulation is needed to see differences in migraine.

593 5.3. Alpha band oscillations

594 There are reports of reduced alpha activity (7-13Hz) contralateral to the aura [150]. Hall *et al.* [151]
595 reported an MEG recording during the spontaneous aura phase of one individual. This recording
596 showed alpha band desynchronisation (a reduction in alpha power) in extrastriate and temporal
597 areas during the time when the observer reported seeing scintillations, and lasting approximately 5
598 minutes. Afterwards, the MEG showed gamma band desynchronisation, for the next 16 minutes, over
599 the inferior temporal lobe. Investigating the EEG at different stages of the migraine attack, Seri *et al.*
600 [152] reported decreased occipital alpha power during an attack in childhood migraine, which was
601 contralateral to the aura hemifield. This was followed by an increase in delta power over bifrontal
602 areas, which spread to the posterior-temporal and occipital areas during the headache. Finally, EEG

603 was normal when recorded interictally. The decrease in alpha contralateral to the hemifield may simply
604 be the reduction in alpha that is seen when an observer views a stimulus - reductions in alpha power
605 have been reported in the case of hallucinations (for a review, see [153]). The normal EEG recorded
606 interictally is typical, and a reason why there is no EEG biomarker for migraine. The increase in delta
607 power seems to be a common theme in EEG recorded during the headache phase of the migraine
608 attack, and this may have significance - in individuals with traumatic brain injury, there has been
609 shown to be an EEG correlate, in the delta band, of intercranially measured spreading depolarisation
610 [35].

611 *5.4. Linking electrophysiology to reaction-diffusion models - oscillations*

612 It may be possible to link oscillatory activity recorded at the scalp to models of migraine aura,
613 in particular for the alpha band. Whilst this was considered the idling rhythm of the brain for a long
614 time, it is now thought that these oscillations have an important role in the inhibition of incoming
615 responses [154]. An individual's alpha band oscillations are thought to act as a "window of excitability"
616 [155]. An incoming signal that coincides with the trough of the alpha oscillation is more likely to be
617 perceived compared to one that coincides with the peak [156]. Alpha band oscillations are thought to
618 be generated in the LGN, with the activity of bursting neurons being synchronised at gap junctions.
619 This results in "relay-mode" spiking - one group of neurons spiking at the peak of the oscillation, and
620 the other group at the trough of the oscillation [157]. Finally, the interneurons provide a cyclic form
621 of suppression to result in alpha band oscillations, which are transmitted through thalamo-cortical
622 neurons into the later visual areas. It is thought that the interneurons and GABA in particular have a
623 relationship with alpha band oscillations, as a recent study showed a positive relationship between
624 alpha band peak frequency and GABA levels [158].

625 When flicker is synchronised to an individual's alpha band oscillations, EEG research has shown
626 that patterns of activity consistent with travelling waves take 2-5s to emerge, compared to 10-15s for
627 trials that are not synchronised to the alpha band oscillations [159]. These travelling waves translate
628 into visual hallucinations such as circles, spirals and grid patterns [159]. There are several reports
629 of visual illusions being elicited by flicker [160]. Illusions are elicited at frequencies specific to the
630 individual, as well as the harmonics of the critical frequency [161]. These hallucinations are also able
631 to be elicited with eyes closed [162], although the strength of the visual stimulus will of course be
632 greatly reduced by the eyelids. It is thought that because the alpha band oscillations are greater with
633 eyes closed, the alpha band may be associated with the hallucinations. However, the flicker rate of the
634 shimmering fortification spectra has been estimated to be around 18Hz [163], which is the range of
635 beta band oscillations.

636 In order to measure the effects of light stimulation without a specific pattern "Ganzfeld" flicker
637 has been used. This essentially incorporates special "glasses" to obscure the visual scene whilst still
638 allowing light through, similar to putting half a table-tennis ball over each eye. Ganzfeld flicker
639 stimulation in non-clinical populations results in radial and spiral hallucinations at lower (5Hz) and
640 higher (17Hz peak) frequencies respectively [164]. When images of these hallucinations were shown
641 to observers, EEG amplitude increased at 4-6Hz for the radial and 11-21Hz for the spiral patterns,
642 linking the hallucination and the frequency of stimulation [164]. Hallucinations induced by flicker in
643 non-clinical populations peaks at 11Hz, and this has been directly modelled using a reaction-diffusion
644 based system of inhibitory and excitatory cell banks (based on the work of [60], which were then
645 passed through a banks of Gabor filters (an energy model) to detect motion [165]. These models
646 shows the relationship between the stimulation frequency and the resulting hallucination. In the stable
647 resting state, in the absence of stimulation, the model displays oscillations at around 13Hz [60]. This
648 is determined by the set of parameters chosen, including the spatial spread (diffusion term) of the
649 inhibitor being greater than the activator. Importantly, in this model there are also time constants for
650 the inhibitor and the activator, which determine the period of the whole system's oscillations. In this
651 case, the time constant for the inhibitor is twice [60], or three times [164] that of the activator. Lower

652 frequency stimulation (around 10Hz) results in hexagonal patterns of cortical activation, which would
653 correspond to chequered hallucinations. Higher frequency stimulation (around 15-20Hz) would result
654 in stripes of cortical activation, which would result in hallucinations such as radial patterns and spirals
655 [60]. These studies include how it is possible to model the hallucinations as a result of the systems
656 ongoing oscillations in combination with a repetitive input.

657 Repetitive visual stimulation, or photic driving, has been of interest in EEG migraine research
658 for a long time, most commonly as an attempt to provide a diagnostic tool that does not rely on
659 self-report. A review of the literature in the 1990s showed the analysis of photic driving responses
660 is not sensitive or specific enough to be used as a diagnostic tool in migraine, however, there was
661 evidence of abnormalities in the photic driving responses in those with migraine above 16Hz [166].
662 Importantly, the authors noted that at the time this had not been linked to the migraine aura, and more
663 recent work has suggested there is no link to migraine aura [167]. A more recent study showed that
664 compared to control groups, both MA and MO showed increased photic driving response for a 2cpd
665 pattern flickered at 10Hz, with MA showing a higher response compared to MO [168]. A 2cpd stimulus
666 flickering at 7.5Hz elicited a greater response in MA compared to MO [169]. Curiously, those with MA
667 showed a weaker response to photic stimulation compared to MO for frequencies of 5, 8, 15, and 20Hz
668 [170]. The lack of conclusive findings make it difficult to draw firm conclusions about the role of photic
669 driving. It is important to note that repetitive visual stimulation can entrain neural responses [171], or
670 at least, evoke repetitive responses (steady-state visual evoked potentials) [172], and the amplitude of
671 these may depend on the frequency of the ongoing oscillations. Future work should first measure the
672 ongoing oscillations as this is likely to impact the amplitude of the response to repetitive visual stimuli.
673 However, the question of how exactly photic stimulation relates to susceptibility to migraine aura is
674 still an open one. Repetitive stimulation can excite the cortex, and entrain oscillations, and so these
675 might be good candidates for possible mechanisms.

676 *5.5. Linking electrophysiology to models - connectivity*

677 It is especially important to consider the ongoing oscillations as these relate to functional
678 connectivity of the brain. It must be noted that recordings of brain activity (whether using EEG
679 or fMRI) are not generally on the same scale as the models - models work on the level of cells,
680 or groups of cells, for example, [50,63] whereas EEG recordings do not have the spatial resolution
681 for this. However recent work has shown that by using networks of reaction-diffusion equations
682 the synchronisation properties of epileptic seizures could be modelled [173]. The synchronisation
683 properties were dependent on global aspects of the network, including the strength of the connectivity
684 between regions. This is important as there is already work available on the effective connectivity in
685 the migraine brain, estimated using EEG after photic stimulation.

686 Estimates of functional connectivity after photic stimulation can discriminate MA and MO. After
687 flash stimulation of 9-27Hz, the amplitude of the response was higher in MA and MO compared to
688 controls over the occipital and parietal channels [174]. Additionally, functional connectivity (Granger
689 causality) in the beta band differentiated between MA, MO and controls [174]. Granger causality is
690 estimated by taking the autoregression of a time series (x) to predict future activity from past activity.
691 This is compared to the autocorrelation from a second time series (y). The error in the prediction
692 from the two time series together is compared to the error in the prediction for the time series x alone.
693 Effective connectivity (based on Granger causality) was higher in MA compared to MO in alpha
694 and beta bands after 5 and 10Hz photic stimulation using 0.5 and 2cpd patterns [175]. Specifically,
695 activity was spread over a larger extent over fronto-central and occipital regions in MA [175], and
696 information is estimated to be flowing posterior to anterior [176]. Granger causality increased with
697 laser stimulation (to cause pain) in those with migraine [177], and Granger causality was increased in
698 migraine in specific areas associated with pain processing [178]. Overall, there is evidence to suggest
699 that information is spreading more readily in migraine from posterior to anterior regions, specifically
700 in alpha and beta bands. This has implications for the models, those areas with increased responses

701 to visual and painful stimuli are propagating information to other regions, resulting in increased
702 responses. It may be possible for models to capture this aspect of rate of information propagation
703 interictally in the migraine brain, which may relate to susceptibility to travelling waves, and the
704 susceptibility of the cortex to precipitating factors.

705 In summary, the migraine aura seems to be characterised by oscillatory differences including
706 pronounced slow wave activity, reduced alpha power, and increased beta power. Factors thought to
707 elicit the migraine attack including hyperventilation, sleep deprivation and photic stimulation have
708 been related to oscillatory differences in EEG. In studies with multiple recordings it appears to be the
709 case that activity normalises after the attack, suggesting that these complex changes are indeed linked
710 to the attack itself. Importantly, recent research has shown fluctuations of oscillatory brain activity
711 (in delta and beta bands) in proximity to migraine attack [179], linking these oscillations to the attack
712 itself more convincingly. Reaction-diffusion models can be used to model the oscillatory behaviour of
713 the system, and in particular, recent work has included a Laplacian function as a diffusion parameter
714 to represent the functional connectivity of the network [61]. Functional connectivity can be estimated
715 from EEG and fMRI recordings, and so this will help to link the theoretical models and the oscillatory
716 behaviour shown experimentally.

717 6. Linking models to psychophysical evidence and signal detection models

718 Behavioural methods can also be used to give indirect estimates of the state of the brain and
719 possible susceptibility to aura. Migraine has been identified as primarily a disorder of sensory
720 processing [28]. As such, some reliable differences in visual perception have been demonstrated
721 in migraine, particularly migraine with aura [180]. These differences show that there are some
722 fundamental differences in the operation of visual processing mechanisms in migraine with aura [180–
723 183], which may be linked to the susceptibility to cortical spreading depression and the hallucinatory
724 experience of visual aura.

725 Basic visual functions have been demonstrated to correlate with GABA levels, for example
726 increased contrast sensitivity with higher GABA levels [184]. Contrast sensitivity is a measure of
727 the overall sensitivity of the visual system to detect visual targets, and is generally found to be
728 lower interictally in migraine, despite the hyperexcitability associated with the condition. There is
729 some evidence that sensitivity is at typical or enhanced levels for small, centrally presented stimuli
730 [182,185–187] when presented without a noise mask, and the overall reduced sensitivity may be linked
731 to patchy impairments of sensitivity across the visual field [188].

732 Orientation discrimination performance has also been shown to relate to GABA levels [189],
733 measured using magnetic resonance spectroscopy, as well as gamma band oscillations [190].
734 Orientation discrimination has been shown to be poorer in migraine compared to controls [191,192].
735 The findings are mixed however, as other research has shown no impairment in orientation
736 discrimination [193], although these authors did show some tentative evidence that the number
737 of migraine aura experienced by participants may relate to orientation discrimination impairments.

738 The relationship between psychophysical tasks and neurotransmitters is not straightforward.
739 For example, surround suppression of motion and binocular rivalry have been shown to relate to
740 GABA levels measured using magnetic resonance spectroscopy [194]. However, contrast surround
741 suppression of a moving stimulus is *increased* in migraine [195]. Yazdani *et al.* [196] assessed two forms
742 of surround suppression, one motion-related, one contrast-related, and found no correlation. This
743 shows that the two types of surround suppression must have independent mechanisms, and so only
744 one, or neither of them, relate to GABA levels. It is possible that only the motion-based surround
745 suppression reflects levels of GABA. A recent study showed no difference between those with migraine
746 and controls in terms of GABA levels, and no difference in terms of performance on binocular rivalry
747 performance [94]. There was also no relationship between either combined glutamate and glutamine,
748 or GABA levels, and binocular rivalry performance [94].

749 Glutamate concentration levels can affect visual task performance. Those with higher levels of
750 Glx show lower motion perception thresholds (more sensitive to motion stimuli) as well as greater
751 fMRI responses [197]. This is again at odds with the migraine literature - those with migraine are
752 thought to have higher levels of glutamate [93], however, a robust behavioural finding is poorer motion
753 perception performance (see [180] for a review). The type of illusory motion perception after viewing
754 a moving stimulus depends on the duration of the priming stimulus as well as individual differences,
755 it could be in either the same direction (assimilation) or the opposite direction (contrast). Using MR to
756 estimate glutamate and GABA levels, the switch between motion assimilation and motion contrast
757 was found to depend on glutamate concentration in the dorsolateral prefrontal cortex. There was no
758 relationship between type of motion perceived and glutamate or GABA levels in either V1 or area
759 MT [198]. This suggests glutamate is not involved in the perception of motion *per se*, but instead the
760 switching of the percept in the higher order areas.

761 Linking the behavioural data to specific neurotransmitters directly is difficult due to the
762 complexity of the system. However, the behavioural data has been interpreted on a more abstract level
763 using signal detection models. For example, some of the most reliable differences in sensory processing
764 in migraine with aura have been found in visual masking. Studies of global motion and form, in which
765 observers detect a global pattern, distributed across many stimulus elements, in the presence of noise,
766 has generally been found to be poorer in migraine [182,183,199]. Tibber *et al.* [200] showed that poorer
767 performance in a mixed migraine group points to a deficit in the ability to detect a target signal while
768 excluding a distracting mask, rather than a more general impairment in the encoding of visual stimuli.
769 These results have been interpreted using signal detection models of visual processing, which specify
770 the gain control on the strength of the initial encoding of visual stimuli, and the presence of noise
771 [182,183,200]. This noise may be additive (independent of the magnitude of the stimulus response)
772 or multiplicative (increasing with the size of the response to the signal). O'Hare and Hibbard [180]
773 concluded that the best account of the hyperexcitation found in migraine, and the psychophysical
774 differences summarised above, is one in which there is an increase in background noise, combined with
775 an increased gain on visual encoding. Both of these characteristics will predispose reaction-diffusion
776 models to the types of hallucinations found in migraine aura, by increasing the likelihood of a short
777 burst of hyper-excitation that would then trigger the larger wave of depolarisation, and are consistent
778 with the physiological differences that are associated with cortical spreading depression.

779 6.1. Differences in performance over the migraine cycle

780 In order to understand migraine aura, it is important to expand knowledge into how performance
781 changes over the course of the migraine cycle. Studies have shown correlations with visual performance
782 and self-reported time since the last attack e.g. [201].

783 Studies investigating just a few time points have also shown differences. Visual field deficits in
784 those with migraine compared to control groups, although quite consistent across time, exhibit some
785 local deficits that may be more pronounced one day after attack [202,203]. When there was a longer (on
786 average) delay after the attack itself no differences in visual field measures were found, although there
787 were differences in electrophysiology rather than psychophysical measures- specifically, steady-state
788 visual evoked responses were higher post-attack compared to interictally [204].

789 Behavioural studies involving multiple testing sessions have also been conducted. McKendrick
790 *et al.* [205] showed that ictal centre-surround suppression (thought to be indicative of cortical inhibition)
791 is stronger in migraine compared to control groups, but this decreases in the days surrounding the
792 attack. Cycle effects have been reported using after-images - after-images are shorter in those with
793 migraine compared to controls, but the duration increases through the migraine cycle, peaking on the
794 day of the headache itself [206]. Subjective unpleasantness ratings for visual and odour stimuli were
795 greater in the headache days compared to interictally, and this was related to increased connectivity in
796 the hypothalamus and brainstem [207].

797 The gold standard for measuring cycle effects is repeat testing throughout *several* migraine cycles,
798 which involves an intensive testing schedule for a long period of time. [Shepherd \[208\]](#) showed interictal
799 global motion performance was poorer in migraine compared to control groups, and that performance
800 improved in the 2 days before and the 2 days after the attack itself. There were no differences in
801 orientation discrimination between groups, and no reliable cycle effects in orientation discrimination
802 performance.

803 Neither signal detection models, nor reaction-diffusion models, currently consider the differences
804 in the migraine cycle. This is an important step for future research, in order to understand the disorder
805 more fully, and be able to devise therapy.

806 6.2. *Linking back to the models*

807 In order to make links between models of migraine aura and psychophysical behaviour and
808 signal detection models, it might seem sensible to start with the parameters that make the network
809 susceptible to spreading depolarisation and subsequent depression. There are several parameters
810 that affect the susceptibility of reaction-diffusion models to travelling waves. One of the main ones is
811 the relative diffusion rates for the activator and the inhibitor. In some of the more complex models,
812 there are non-linear equations for the reaction component, which can also effect the susceptibility
813 to travelling waves e.g. [\[41\]](#). Given the number of possible neurochemical mechanisms that could
814 possibly be represented by the different parameters, identifying the correct ones in those with migraine
815 is not trivial. This might be leaving the reader wondering if there is any point to all these models at all.
816 The issue here may be the level of abstraction: instead of thinking at the level of neurotransmitters, it
817 may be more worthwhile to look at the level of measurable behaviour to link this to the models. There
818 are possibilities for doing this in terms of EEG estimates of functional connectivity for example. This
819 has been started in recent work in epilepsy, and may be a fruitful area when considering migraine
820 [\[149\]](#).

821 It may also be possible to link the models of aura to visual performance from these individuals,
822 throughout the migraine cycle if possible. For example, signal detection theory has been used to
823 account for behavioural data with some success in migraine e.g. [\[182,183\]](#). It has been suggested in
824 the case of those with migraine aura, that there will be a particular susceptibility to external stimuli
825 due to increased internal noise levels, thought to be due to increased spontaneous neural firing rates
826 [\[180\]](#). One outstanding question in migraine aura is what initiates the migraine aura in the first place.
827 One possibility is input to the system, in the form of triggers, however, triggers are idiosyncratic and
828 have been demonstrated to be unreliable [\[109\]](#). In the original reaction-diffusion model, the initiation
829 of the pattern formation was due to spontaneous fluctuations of activity [\[46\]](#). This could provide
830 an important bridge between reaction-diffusion systems modelling aura and signal detection theory
831 modelling behaviour - both would predict increased levels of spontaneous firing, which would make
832 the initiation of an attack (all other things being equal) more likely.

833 In order to link models to perceptual performance, it is important to understand which elements
834 of the models relate to perception. It has been suggested that the output of the pyramidal cells relates
835 to our perceptual experience [\[50\]](#). The idea of where perception happens is beyond the scope of this
836 review, but it is important to note, the model outputs generally plotted are the excitatory system at
837 that particular time point (e.g. [\[54\]](#)), which could be the output of (groups of) pyramidal cells. Neural
838 oscillations, specifically alpha band oscillations, have been directly linked to perceptual performance.
839 For example, observers are more likely to detect a stimulus if its arrival coincides with the trough
840 of the alpha band oscillation (low alpha power), however the arrival of the incoming stimulus has
841 the effect of increasing phase locking (synchronisation) of the alpha band oscillations and therefore
842 increasing the resulting ERP component [\[209–211\]](#). Those with migraine aura also show an increase
843 in ERP response amplitude to incoming stimuli compared to controls [\[125,212,213\]](#), which would be
844 consistent with this idea, however they show *increased* lower alpha band (8-10Hz) power in the resting
845 state compared to controls [\[214\]](#). These recordings were all taken interictally, and so given that the

846 alpha band reduces during the attack [151,152], it is essential to look at cycle effects in the EEG before
847 drawing firm conclusions.

848 This is a relatively unexplored area but it might help to use these models of the migraine aura
849 in combination with experimental results on EEG behaviour during an attack and behavioural
850 performance during the migraine cycle to help understand how attacks are initiated, which may
851 help with preventing them.

852 7. Discussion and Unresolved Questions

853 This review outlines reaction-diffusion models of the classic features of migraine aura, the zig-zag
854 fortifications and the scotoma. These reaction-diffusion models of inhibitory and excitatory interactions
855 between networks of neurons are flexible abstractions that help understand the dynamics of the
856 cortical spreading depolarisation and depression, respectively. Factors predisposing models to cortical
857 spreading depolarisation and depression are (1) the balance between strength and spatial range of
858 excitatory and inhibitory interactions and (2) the likelihood of occurrence of spontaneous hyperactivity
859 which could trigger wave of depolarisation. Direct links to electrophysiology are difficult due to the
860 lack of experimental data during the attack, however, neural oscillations may be a fruitful area of
861 investigation as these relate to functional connectivity of the network, and the excitability of the brain,
862 which may relate to the terms of the models. Additionally, neural oscillations have been shown to
863 fluctuate over the migraine cycle, linking them to the disorder. Recent advances in wearable technology
864 may open possibilities for investigating oscillatory behaviour and functional connectivity estimates
865 throughout the migraine cycle, which would be able to directly link to the models. For example,
866 wearable technology has been used to estimate electrophysiological activity at different stages of the
867 migraine cycle [179,215].

868 Psychophysical methods can also be used to determine the relevant parameters for the models,
869 as these provide indirect estimates of cortical excitability. For example, signal detection models
870 accounting for perceptual performance predict increased noise and gain in the migraine brain. These
871 may relate to reaction-diffusion model parameters, e.g. internal noise levels may relate to the initial
872 random fluctuation in activity that initiates the travelling waves in the models. Importantly, perceptual
873 performance varies over the migraine cycle, which would be expected if the underlying processes
874 relate to the disorder itself.

875 7.1. Arguments against cortical spreading depression as the mechanism for migraine

876 Importantly, there are several arguments against describing migraine aura through cortical
877 spreading depression and models thereof (see [216] and [217] for detailed discussion). Firstly, cortical
878 spreading depression has been robustly recorded for patients who have experienced a stroke or head
879 trauma [35,218] where it is possible to obtain continuous electrocortical recording via cortical electrodes
880 or subcortical electrocorticograms. In contrast, to date there is no electrophysiological evidence of
881 spreading depression during a human migraine attack.

882 There are also questions about how cortical spreading depression accounts for more complex aura
883 and hallucinations. For example bilateral visual aura, which are experienced across both hemispheres
884 are not explained by cortical spreading depression, since propagation requires contiguous grey matter
885 and does not cross the corpus callosum [217]. Since spreading depression only propagates in the
886 hemisphere of origin it is also argued [216] to insufficiently account for the bilateral pain experienced
887 by 40% of people with migraine.

888 Thus, it is important to note that the models are an oversimplification of the diversity of migraine
889 aura, and at present the models focus on the typical, simple geometric hallucinations. There are
890 more complex hallucinations such as hallucinations of people and objects e.g. [9]. which tend to be
891 idiosyncratic and less common than the typical zigzag lines, flashing lights and scintillating scotoma
892 [8,9]. These more advanced illusions are not included in the current models and complex patterns

893 may be a result of a secondary involvement of higher visual areas of the brain, such as those areas
894 specialised for face and object recognition.

895 Migraine is a multi faceted disorder and there is also variation in an individual's attacks. The
896 models present a simplification of one possible set of events, and do not take this variability into
897 account. Models currently limit themselves on the propagation of the travelling wave, rather than
898 inferences about the possible hallucinations if it were to spread to higher order visual areas. However,
899 recent work by Kroos *et al.* [219] has generated individual-specific reaction-diffusion models using the
900 individual's MRI data. This model successfully recreates the diffusion of water as an approximation
901 of electrical conductivity, and importantly, the shape of the individual's cortex is incorporated in
902 modelling the spreading depression for that individual. This is important as it is the first step to
903 modelling the individual-specific variation in aura.

904 *7.2. Can we infer clues to aura susceptibility from the models?*

905 One outstanding question is whether there are behavioural and electrophysiological clues to
906 aura susceptibility, and this might be able to be predicted from the models. For example, alpha
907 band oscillations relate to the inhibition of responses, which may facilitate the spread of the migraine
908 aura. Increased internal noise may also relate to the susceptibility to migraine aura, and this could
909 be measured using behavioural techniques. Predictions about internal noise levels could be made
910 based on varying model parameters, generating clear, testable hypotheses. Given the difficulty of
911 direct physiological measures during the migraine aura, it may be possible to use psychophysical
912 measures with well-established hypotheses, to provide a better route to understanding altered sensory
913 processing.

914 *7.3. How the models account for pain*

915 Another unresolved element is the link to the headache and pain of migraine. It is common to
916 experience migraine headache without aura, and it is also possible to experience aura without pain.
917 Some approaches consider migraine without aura as intermediate, between attacks with aura and
918 no attack. The reaction-diffusion models are limited to the aura, and do not explicitly account for
919 pain. However, Kroos *et al.* [220] recently applied a reaction-diffusion equation to model spreading
920 depression for five single case studies of patients with migraine. Simulated spreading depression was
921 personalised for each patient matching their symptoms during a migraine attack to the wavefront
922 propagation, based on acquired MRI data. In the simulation the spreading depression reached
923 the primary and secondary somatosensory cortex, specifically the topographical area related to the
924 trigeminal nerve, and pain processing prefrontal areas. The authors suggest that the propagation of
925 extracellular K⁺ may elicit the headache by activating afferent pain receptors [220]. This is important
926 as the spreading depression is linked to the activation of the trigeminal neurons that are involved in
927 mediating lateralised head pain [217]. Future work to link the spreading depression and the head pain
928 could use reaction-diffusion models as a basis.

929 *7.4. Long term effects and stroke risk*

930 There is also the possibility of long-term effects of migraine. It has been suggested that repeated
931 migraine attacks increase the likelihood of subsequent migraine attacks (for a review, see [221]).
932 Frequency of attacks can increase in some individuals, eventually even progressing to chronic migraine,
933 and this may be due to sensitisation of the system from repeated spreading depolarisation and
934 depression mechanism [222]. Although migraine is thought to be benign [223] and the attacks fully
935 reversible [224], there is some evidence of possible long-term damage from regular attacks [2,225–227].
936 There is also an increased risk of stroke in those with migraine aura [228]. Stroke is also thought to be
937 a disorder as a result of spreading depolarisation [218,229], and so this is an important avenue to be
938 explored in terms of models of spreading depolarisation and depression.

939 7.5. Age and sex differences

940 The majority of the literature in this review is focused on adults with migraine aura, and therefore
941 the conclusions must be restricted to this population. However, it is important to consider those with
942 paediatric migraine as well. The prevalence of paediatric migraine overall is around 8%, and around
943 half continue to experience migraine into adulthood [230]. However, the prevalence of paediatric
944 migraine aura is much lower, estimated to be around 1.6% [231]. The clinical characteristics are similar
945 to those of adults, with the majority experiencing visual aura, and this is stable across the age bands
946 investigated (under 6, 7-10, 11-14, and over 15 years) [232].

947 There are also sex differences in migraine, migraine being more prevalent in females than males,
948 and this interacts with age. Across the age range 3 to 85+ years, migraine prevalence is estimated to be
949 17% in females compared to 8% in males, with the ratio females to males being the greatest between
950 the ages of 20-40 [233]. However, under the age of 10, female and male prevalence was found to be
951 similar [233]. Research has shown the median age of onset is estimated to be mid-twenties for both
952 men and women, suggesting that puberty is not a factor in determining migraine [234].

953 Hormonal changes have been thought to be the cause of the increased prevalence in migraine
954 in females compared to males. However, there are differences between migraine with and without
955 aura - attacks without aura are more likely with the withdrawal of oestrogen, whereas migraine
956 with aura attacks are more likely when there are high levels of oestrogen, for example pregnancy
957 [235]. Diary studies have shown that migraine occurs around the onset of menstruation in those with
958 migraine without aura, but not migraine with aura [236], and higher peaks in oestrogen levels across
959 the menstrual cycle have been found in migraine with aura [235]. Additionally, systematic reviews of
960 the literature have found that migraine without aura seems to be more affected by the transition of
961 menopause compared to migraine with aura, which seems to be more stable [237,238]. Research has
962 shown that migraine aura is not related to the menopause [239].

963 The current models do not consider any age-related or sex-related differences at present, but this
964 could potentially be incorporated in future. For example, it has been proposed that visual arousal
965 might be increased around the peak in oestrogen levels prior to ovulation [240]. The higher peaks
966 in oestrogen level in migraine with aura might thus be associated with increased excitability in the
967 visual cortex. While some studies have suggested an increase in visual sensitivity around ovulation
968 [241-247], others have shown no effects on contrast sensitivity [248]. It would however be informative
969 to study this directly in cases of migraine with aura.

970 Interestingly, it has been shown that spreading depolarisation cannot be elicited using K⁺ in the
971 neonatal rat before the age of 12 days [249]. Understanding the factors that protect the juvenile brain
972 from spreading depolarisation is of interest for the progression of migraine, and worth exploring in
973 future modelling work.

974 8. Conclusion

975 This review has outlined reaction-diffusion models for a general readership, with the aim
976 of improving accessibility to the diverse disciplines involved in understanding migraine. Direct
977 experimental literature supporting these models is sparse, since measurements during the attack
978 are logistically difficult. Ideally, intercranial recordings during the aura under different conditions
979 would provide measures of the cortical dynamics of cortical spreading depolarisation and depression,
980 however such measures are not possible. In order to treat migraine, we need to know the mechanisms
981 of the aura and, perhaps more importantly, the factors determining susceptibility to attacks. This is
982 where reaction-diffusion models could be useful to bridge the gap between proposed mechanisms and
983 testable hypotheses, since they are able to illuminate the "black box" of what is happening during the
984 aura itself, and develop hypotheses that can be tested using electrophysiological and psychophysical
985 techniques. It would be especially useful to track the changes in model parameters and compare to
986 experimental data across the migraine cycle. With longitudinal behavioural evidence becoming easier

987 to obtain through advances in wearable technology, the theoretical predictions of these models will be
988 testable in the near future.

989 **Funding:** This research received no external funding.

990 **Acknowledgments:**

991 **Conflicts of Interest:** The authors declare no conflict of interest.

992 **Abbreviations**

993 The following abbreviations are used in this manuscript:

994	AC	Alternating current
	BAM	Basilar-type-migraine
	DC	Direct current
	GABA	Gamma-aminobutyric acid
	Glx	Combined glutamate and glutamine complex
	K+	Potassium ion
	MA	Migraine-with-aura
	MEG	Magnetoencephalogram
	MO	Migraine-without-aura
995	MR	Magnetic resonance
	MT	Middle-temporal
	NDMA	Nitrosodimethylamine
	PSD	Power spectral density
	rCBF	Cerebral blood flow
	tACS	transcranial alternating current stimulation
	tDCS	transcranial direct current stimulation
	TMS	transcranial magnetic stimulation
	Xe	xenon

996 **References**

- 997 1. Kelman, L. The aura: a tertiary care study of 952 migraine patients. *Cephalalgia* **2004**, *24*, 728–734.
998 doi:10.1111/j.1468-2982.2004.00748.x.
- 999 2. Smith, J.M.; Bradley, D.P.; James, M.F.; Huang, C.L.H. Physiological studies of cortical spreading depression.
1000 *Biological Reviews* **2006**, *81*, 457–481.
- 1001 3. Teeple, R.C.; Caplan, J.P.; Stern, T.A. Visual hallucinations: differential diagnosis and treatment. *Primary*
1002 *Care Companion to the Journal of Clinical Psychiatry* **2009**, *11*, 26.
- 1003 4. Steiner, T.; Scher, A.; Stewart, W.; Kolodner, K.; Liberman, J.; Lipton, R. The prevalence and disability
1004 burden of adult migraine in England and their relationships to age, gender and ethnicity. *Cephalalgia* **2003**,
1005 *23*, 519–527. doi:10.1046/j.1468-2982.2003.00568.x.
- 1006 5. Viana, M.; Sances, G.; Linde, M.; Ghiotto, N.; Guaschino, E.; Allena, M.; Terrazzino, S.; Nappi, G.;
1007 Goadsby, P.J.; Tassorelli, C. Clinical features of migraine aura: results from a prospective diary-aided study.
1008 *Cephalalgia* **2017**, *37*, 979–989. doi:https://doi.org/10.1177/0333102416657147.
- 1009 6. Viana, M.; Sprenger, T.; Andelova, M.; Goadsby, P.J. The typical duration of migraine aura: a systematic
1010 review. *Cephalalgia* **2013**, *33*, 483–490.
- 1011 7. Viana, M.; Sances, G.; Linde, M.; Nappi, G.; Khaliq, F.; Goadsby, P.J.; Tassorelli, C. Prolonged migraine
1012 aura: new insights from a prospective diary-aided study. *The journal of headache and pain* **2018**, *19*, 1–5.
- 1013 8. Queiroz, L.P.; Friedman, D.I.; Rapoport, A.M.; Purdy, R.A. Characteristics of migraine visual aura in
1014 Southern Brazil and Northern USA. *Cephalalgia* **2011**, *31*, 1652–1658. doi:10.1177/0333102411430263.
- 1015 9. Viana, M.; Tronvik, E.A.; Do, T.P.; Zecca, C.; Hougaard, A. Clinical features of visual migraine aura: a
1016 systematic review. *The journal of headache and pain* **2019**, *20*, 64. doi:10.1186/s10194-019-1008-x.
- 1017 10. Plant, G.T. The fortification spectra of migraine. *British medical journal (Clinical research ed.)* **1986**, *293*, 1613.
1018 doi:https://www.bmj.com/content/bmj/293/6562/1613.full.pdf.
- 1019 11. Sacks, O. Migraine. Berkeley, 1992.
- 1020 12. Schott, G. Exploring the visual hallucinations of migraine aura: the tacit contribution of illustration. *Brain*
1021 **2007**, *130*, 1690–1703. doi:https://doi.org/10.1093/brain/awl348.

- 1022 13. Lashley, K.S. Patterns of cerebral integration indicated by the scotomas of migraine. *Archives of Neurology & Psychiatry* **1941**, *46*, 331–339. doi:10.1001/archneurpsyc.1941.02280200137007.
- 1023
- 1024 14. Panayiotopoulos, C. Elementary visual hallucinations in migraine and
1025 epilepsy. *Journal of Neurology, Neurosurgery & Psychiatry* **1994**, *57*, 1371–1374.
1026 doi:https://www.ncbi.nlm.nih.gov/pmc/articles/PMC1073189/pdf/jnnpsyc00041-0069.pdf.
- 1027 15. Martínez, J.V.L.; Speciali, J.G. Migraine with visual aura versus occipital epilepsy. *Headache: The Journal of*
1028 *Head and Face Pain: Letters to the Editor* **1997**, *37*, 113–113. doi:10.1046/j.1526-4610.1997.3702113.x.
- 1029 16. Panayiotopoulos, C. Elementary visual hallucinations, blindness, and headache in idiopathic occipital
1030 epilepsy: differentiation from migraine. *Journal of Neurology, Neurosurgery & Psychiatry* **1999**, *66*, 536–540.
1031 doi:http://dx.doi.org/10.1136/jnnp.66.4.536.
- 1032 17. Panayiotopoulos, C.P. Visual aura of migraine versus visual occipital lobe seizures. *Cephalalgia* **2012**,
1033 *32*, 654–654. doi:10.1177/0333102412443332.
- 1034 18. Sturzenegger, M.H.; Meienberg, O. Basilar artery migraine: A follow-up study of 82 cases. *Headache: The*
1035 *Journal of Head and Face Pain* **1985**, *25*, 408–415.
- 1036 19. Siegel, R.K. Cocaine hallucinations. *The American journal of psychiatry* **1978**.
- 1037 20. Dybowski, M. *Conditions for the appearance of hypnagogic visions*; Poznanskie Towarzystwo Psychologiczne,
1038 1939.
- 1039 21. Ermentrout, G.B.; Cowan, J.D. A mathematical theory of visual hallucination patterns. *Biological cybernetics*
1040 **1979**, *34*, 137–150.
- 1041 22. Eriksen, M.; Thomsen, L.; Andersen, I.; Nazim, F.; Olesen, J. Clinical characteristics of 362 patients with
1042 familial migraine with aura. *Cephalalgia* **2004**, *24*, 564–575. doi:10.1111/j.1468-2982.2003.00718.x.
- 1043 23. Hansen, J.M.; Baca, S.M.; VanValkenburgh, P.; Charles, A. Distinctive anatomical and physiological features
1044 of migraine aura revealed by 18 years of recording. *Brain* **2013**, *136*, 3589–3595.
- 1045 24. Bowyer, S.; Tepley, N.; Papuashvili, N.a.; Kato, S.; Barkley, G.; Welch, K.; Okada, Y. Analysis of MEG
1046 signals of spreading cortical depression with propagation constrained to a rectangular cortical strip: II.
1047 Gyrencephalic swine model. *Brain research* **1999**, *843*, 79–86.
- 1048 25. Hadjikhani, N.; Del Rio, M.S.; Wu, O.; Schwartz, D.; Bakker, D.; Fischl, B.; Kwong, K.K.; Cutrer, F.M.; Rosen,
1049 B.R.; Tootell, R.B.; others. Mechanisms of migraine aura revealed by functional MRI in human visual
1050 cortex. *Proceedings of the national academy of sciences* **2001**, *98*, 4687–4692.
- 1051 26. Dreier, J.P. Spreading depolarization, Tsunami im Hirn. *e-Neuroforum* **2009**, *15*, 108–113.
- 1052 27. Dreier, J.P.; Major, S.; Foreman, B.; Winkler, M.K.; Kang, E.J.; Milakara, D.; Lemale, C.L.; DiNapoli, V.;
1053 Hinzman, J.M.; Woitzik, J.; others. Terminal spreading depolarization and electrical silence in death of
1054 human cerebral cortex. *Annals of neurology* **2018**, *83*, 295–310.
- 1055 28. Goadsby, P.J.; Holland, P.R.; Martins-Oliveira, M.; Hoffmann, J.; Schankin, C.; Akerman, S. Pathophysiology
1056 of migraine: a disorder of sensory processing. *Physiological reviews* **2017**.
- 1057 29. Leo, A.A. Pial circulation and spreading depression of activity in the cerebral cortex. *Journal of*
1058 *Neurophysiology* **1944**, *7*, 391–396.
- 1059 30. Leao, A.A. Spreading depression of activity in the cerebral cortex. *Journal of neurophysiology* **1944**, *7*, 359–390.
- 1060 31. Lauritzen, M.; Dreier, J.P.; Fabricius, M.; Hartings, J.A.; Graf, R.; Strong, A.J. Clinical relevance of cortical
1061 spreading depression in neurological disorders: migraine, malignant stroke, subarachnoid and intracranial
1062 hemorrhage, and traumatic brain injury. *Journal of Cerebral Blood Flow & Metabolism* **2011**, *31*, 17–35.
- 1063 32. Wilkinson, F. Auras and other hallucinations: windows on the visual brain. *Progress in brain research* **2004**,
1064 *144*, 305–320.
- 1065 33. Dahlem, M.A.; Müller, S. Migraine aura dynamics after reverse retinotopic mapping of weak excitation
1066 waves in the primary visual cortex. *Biological cybernetics* **2003**, *88*, 419–424.
- 1067 34. Charles, A.; Brennan, K. Cortical spreading depression—new insights and persistent questions. *Cephalalgia*
1068 **2009**, *29*, 1115–1124.
- 1069 35. Hartings, J.A.; Wilson, J.A.; Hinzman, J.M.; Pollandt, S.; Dreier, J.P.; DiNapoli, V.; Ficker, D.M.; Shutter,
1070 L.A.; Andaluz, N. Spreading depression in continuous electroencephalography of brain trauma. *Annals of*
1071 *neurology* **2014**, *76*, 681–694.
- 1072 36. Charles, A.C.; Baca, S.M. Cortical spreading depression and migraine. *Nature Reviews Neurology* **2013**,
1073 *9*, 637.

- 1074 37. Hofmeijer, J.; Van Kaam, C.; van de Werff, B.; Vermeer, S.E.; Tjepkema-Cloostermans, M.C.; van Putten,
1075 M.J. Detecting cortical spreading depolarization with full band scalp electroencephalography: an illusion?
1076 *Frontiers in neurology* **2018**, *9*, 17.
- 1077 38. Harriott, A.M.; Takizawa, T.; Chung, D.Y.; Chen, S.P. Spreading depression as a preclinical model of
1078 migraine. *The journal of headache and pain* **2019**, *20*, 1–12.
- 1079 39. Billock, V.A.; Tsou, B.H. Elementary visual hallucinations and their relationships to neural pattern-forming
1080 mechanisms. *Psychological bulletin* **2012**, *138*, 744.
- 1081 40. Zandt, B.J.; ten Haken, B.; van Putten, M.J.; Dahlem, M.A. How does spreading depression spread?
1082 Physiology and modeling. *Reviews in the Neurosciences* **2015**, *26*, 183–198.
- 1083 41. Dahlem, M.A.; Hadjikhani, N. Migraine aura: retracting particle-like waves in weakly susceptible cortex.
1084 *PLoS One* **2009**, *4*, e5007.
- 1085 42. Dahlem, M.A.; Müller, S.C. Self-induced splitting of spiral-shaped spreading depression waves in chicken
1086 retina. *Experimental brain research* **1997**, *115*, 319–324.
- 1087 43. Wilson, H.R.; Cowan, J.D. Excitatory and inhibitory interactions in localized populations of model neurons.
1088 *Biophysical journal* **1972**, *12*, 1–24.
- 1089 44. Wilson, H.R.; Cowan, J.D. A mathematical theory of the functional dynamics of cortical and thalamic
1090 nervous tissue. *Kybernetik* **1973**, *13*, 55–80.
- 1091 45. Turing, A. The chemical basis of morphogenesis. *Philosophical Transactions of the Royal Society of London*
1092 **1952**, B237 (641).
- 1093 46. Kondo, S.; Miura, T. Reaction-diffusion model as a framework for understanding biological pattern
1094 formation. *science* **2010**, *329*, 1616–1620.
- 1095 47. Gray, P.; Scott, S.K. *Chemical oscillations and instabilities: non-linear chemical kinetics*; Clarendon Press, Oxford,
1096 1990.
- 1097 48. Garrity, M. How the tiger got its stripes. [https://blogs.mathworks.com/graphics/2015/03/16/how-the-
1098 tiger-got-its-stripes/](https://blogs.mathworks.com/graphics/2015/03/16/how-the-tiger-got-its-stripes/). Accessed: 2021-02-27.
- 1099 49. Gierer, A.; Meinhardt, H. A theory of biological pattern formation. *Kybernetik* **1972**, *12*, 30–39.
- 1100 50. Zhaoping, L.; Li, Z. *Understanding vision: theory, models, and data*; Oxford University Press, USA, 2014.
- 1101 51. Tass, P. Oscillatory Cortical Activity during Visual Hallucinations. *Journal of biological physics* **1997**,
1102 *23*, 21–66.
- 1103 52. Reggia, J.A.; Montgomery, D. A computational model of visual hallucinations in migraine. *Computers in*
1104 *biology and medicine* **1996**, *26*, 133–141.
- 1105 53. Dahlem, M.; Engelmann, R.; Löwel, S.; Müller, S. Does the migraine aura reflect cortical organization?
1106 *European Journal of Neuroscience* **2000**, *12*, 767–770.
- 1107 54. Dahlem, M.; Chronicle, E. A computational perspective on migraine aura. *Progress in neurobiology* **2004**,
1108 *74*, 351–361.
- 1109 55. Dahlem, M.A.; Müller, S.C. Reaction-diffusion waves in neuronal tissue and the window of cortical
1110 excitability. *Annalen der Physik* **2004**, *13*, 442–449.
- 1111 56. Field, D.J.; Hayes, A.; Hess, R.F. Contour integration by the human visual system: evidence for a local
1112 “association field”. *Vision research* **1993**, *33*, 173–193.
- 1113 57. Blasdel, G.; Obermayer, K.; Kiorpes, L. Organization of ocular dominance and orientation columns in the
1114 striate cortex of neonatal macaque monkeys. *Visual neuroscience* **1995**, *12*, 589–603.
- 1115 58. Daugman, J.G. Uncertainty relation for resolution in space, spatial frequency, and orientation optimized
1116 by two-dimensional visual cortical filters. *JOSA A* **1985**, *2*, 1160–1169.
- 1117 59. Field, D.J. What is the goal of sensory coding? *Neural computation* **1994**, *6*, 559–601.
- 1118 60. Rule, M.; Stoffregen, M.; Ermentrout, B. A model for the origin and properties of flicker-induced geometric
1119 phosphenes. *PLoS Comput Biol* **2011**, *7*, e1002158.
- 1120 61. Atasoy, S.; Donnelly, I.; Pearson, J. Human brain networks function in connectome-specific harmonic
1121 waves. *Nature communications* **2016**, *7*, 10340.
- 1122 62. Siddiqui, M.S.M.; Bhaumik, B. A reaction-diffusion model to capture disparity selectivity in primary visual
1123 cortex. *PloS one* **2011**, *6*, e24997.
- 1124 63. Seriès, P.; Latham, P.E.; Pouget, A. Tuning curve sharpening for orientation selectivity: coding efficiency
1125 and the impact of correlations. *Nature neuroscience* **2004**, *7*, 1129–1135.

- 1126 64. Dahlem, Y.A.; Dahlem, M.A.; Mair, T.; Braun, K.; Müller, S.C. Extracellular potassium alters frequency and
1127 profile of retinal spreading depression waves. *Experimental brain research* **2003**, *152*, 221–228.
- 1128 65. Hauge, A.W.; Kirchmann, M.; Olesen, J. Characterization of consistent triggers of migraine with aura.
1129 *Cephalalgia* **2011**, *31*, 416–438.
- 1130 66. Kilic, K.; Karatas, H.; Dönmez-Demir, B.; Eren-Kocak, E.; Gursoy-Ozdemir, Y.; Can, A.; Petit, J.M.;
1131 Magistretti, P.J.; Dalkara, T. Inadequate brain glycogen or sleep increases spreading depression
1132 susceptibility. *Annals of neurology* **2018**, *83*, 61–73.
- 1133 67. Rasmussen, R.; Nicholas, E.; Petersen, N.C.; Dietz, A.G.; Xu, Q.; Sun, Q.; Nedergaard, M. Cortex-wide
1134 changes in extracellular potassium ions parallel brain state transitions in awake behaving mice. *Cell reports*
1135 **2019**, *28*, 1182–1194.
- 1136 68. Olesen, J.; Bes, A.; Kunkel, R.; Lance, J.W.; Nappi, G.; Pfaffenrath, V.; Rose, F.C.; Schoenberg, B.S.; Soyka, D.;
1137 Tfelt-Hansen, P.; others. The international classification of headache disorders, (beta version). *Cephalalgia*
1138 **2013**, *33*, 629–808.
- 1139 69. Hounsgaard, J.; Nicholson, C. Potassium accumulation around individual purkinje cells in cerebellar slices
1140 from the guinea-pig. *The Journal of physiology* **1983**, *340*, 359–388.
- 1141 70. Hertz, L.; Chen, Y. Importance of astrocytes for potassium ion (K⁺) homeostasis in brain and glial effects
1142 of K⁺ and its transporters on learning. *Neuroscience & Biobehavioral Reviews* **2016**, *71*, 484–505.
- 1143 71. Major, S.; Huo, S.; Lemale, C.L.; Siebert, E.; Milakara, D.; Woitzik, J.; Gertz, K.; Dreier, J.P.
1144 Direct electrophysiological evidence that spreading depolarization-induced spreading depression is the
1145 pathophysiological correlate of the migraine aura and a review of the spreading depolarization continuum
1146 of acute neuronal mass injury. *GeroScience* **2020**, *42*, 57–80.
- 1147 72. Somjen, G.G. Mechanisms of spreading depression and hypoxic spreading depression-like depolarization.
1148 *Physiological reviews* **2001**, *81*, 1065–1096.
- 1149 73. van den Maagdenberg, A.M.; Pietrobon, D.; Pizzorusso, T.; Kaja, S.; Broos, L.A.; Cesetti, T.; van de Ven,
1150 R.C.; Tottene, A.; van der Kaa, J.; Plomp, J.J.; others. A *Cacna1a* knockin migraine mouse model with
1151 increased susceptibility to cortical spreading depression. *Neuron* **2004**, *41*, 701–710.
- 1152 74. Turner, T.J.; Adams, M.E.; Dunlap, K. Calcium channels coupled to glutamate release identified by
1153 omega-Aga-IVA. *Science* **1992**, *258*, 310–313.
- 1154 75. Timmermann, D.B.; Westenbroek, R.E.; Schousboe, A.; Catterall, W.A. Distribution of
1155 high-voltage-activated calcium channels in cultured γ -aminobutyric acidergic neurons from mouse cerebral
1156 cortex. *Journal of neuroscience research* **2002**, *67*, 48–61.
- 1157 76. Dietzel, I.; Heinemann, U.; Hofmeier, G.; Lux, H. Stimulus-induced changes in extracellular Na⁺ and Cl⁻
1158 concentration in relation to changes in the size of the extracellular space. *Experimental brain research* **1982**,
1159 *46*, 73–84.
- 1160 77. Mueller, M.; Somjen, G.G. Na⁺ and K⁺ concentrations, extra-and intracellular voltages, and the effect of
1161 TTX in hypoxic rat hippocampal slices. *Journal of neurophysiology* **2000**, *83*, 735–745.
- 1162 78. Barolet, A.; Morris, M. Changes in extracellular K⁺ evoked by GABA, THIP and baclofen in the guinea-pig
1163 hippocampal slice. *Experimental brain research* **1991**, *84*, 591–598.
- 1164 79. DiNuzzo, M.; Mangia, S.; Maraviglia, B.; Giove, F. Physiological bases of the K⁺ and the glutamate/GABA
1165 hypotheses of epilepsy. *Epilepsy research* **2014**, *108*, 995–1012.
- 1166 80. Van Harreveld, A.; Stamm, J. Cortical responses to metrazol and sensory stimulation in the rabbit.
1167 *Electroencephalography and clinical neurophysiology* **1955**, *7*, 363–370.
- 1168 81. Palmer, J.; Chronicle, E.; Rolan, P.; Mulleners, W. Cortical hyperexcitability is cortical under-inhibition:
1169 evidence from a novel functional test of migraine patients. *Cephalalgia* **2000**, *20*, 525–532.
- 1170 82. Mulleners, W.M.; Chronicle, E.; Vredeveld, J.; Koehler, P. Visual cortex excitability in migraine before and
1171 after valproate prophylaxis: a pilot study using TMS. *European journal of neurology* **2002**, *9*, 35–40.
- 1172 83. Kurcyus, K.; Annac, E.; Hanning, N.M.; Harris, A.D.; Oeltzschner, G.; Edden, R.; Riedl, V. Opposite
1173 dynamics of GABA and glutamate levels in the occipital cortex during visual processing. *Journal of*
1174 *Neuroscience* **2018**, *38*, 9967–9976.
- 1175 84. Dreier, J.P.; Major, S.; Pannek, H.W.; Woitzik, J.; Scheel, M.; Wiesenthal, D.; Martus, P.; Winkler, M.K.;
1176 Hartings, J.A.; Fabricius, M.; others. Spreading convulsions, spreading depolarization and epileptogenesis
1177 in human cerebral cortex. *Brain* **2012**, *135*, 259–275.

- 1178 85. Bigal, M.; Hetherington, H.; Pan, J.; Tsang, A.; Grosberg, B.; Avdievich, N.; Friedman, B.; Lipton, R.
1179 Occipital levels of GABA are related to severe headaches in migraine. *Neurology* **2008**, *70*, 2078–2080.
- 1180 86. Stærnøse, T.G.; Knudsen, M.K.; Kasch, H.; Blicher, J.U. Cortical GABA in migraine with aura—an ultrashort
1181 echo magnetic resonance spectroscopy study. *The Journal of Headache and Pain* **2019**, *20*, 110.
- 1182 87. Bridge, H.; Stagg, C.J.; Near, J.; Lau, C.I.; Zisner, A.; Cader, M.Z. Altered neurochemical coupling in the
1183 occipital cortex in migraine with visual aura. *Cephalalgia* **2015**, *35*, 1025–1030.
- 1184 88. Aguila, M.E.R.; Rebeck, T.; Leaver, A.M.; Lagopoulos, J.; Brennan, P.C.; Hübscher, M.; Refshauge, K.M.
1185 The association between clinical characteristics of migraine and brain GABA levels: an exploratory study.
1186 *The Journal of Pain* **2016**, *17*, 1058–1067.
- 1187 89. D’Andrea, G.; Granella, F.; Cataldini, M.; Verdelli, F.; Balbi, T. GABA and glutamate in migraine. *The*
1188 *Journal of Headache and Pain* **2001**, *2*, s57–s60.
- 1189 90. Chronicle, E.P.; Mulleners, W.M. Anticonvulsant drugs for migraine prophylaxis. *Cochrane Database of*
1190 *Systematic Reviews* **2004**, *3*. doi:10.1002/14651858.CD003226.pub2.
- 1191 91. Cai, K.; Nanga, R.P.; Lamprou, L.; Schinstine, C.; Elliott, M.; Hariharan, H.; Reddy, R.; Epperson, C.N. The
1192 impact of gabapentin administration on brain GABA and glutamate concentrations: a 7T 1H-MRS study.
1193 *Neuropsychopharmacology* **2012**, *37*, 2764–2771.
- 1194 92. Linde, M.; Mulleners, W.M.; Chronicle, E.P.; McCrory, D.C. Gabapentin or pregabalin for the
1195 prophylaxis of episodic migraine in adults. *Cochrane Database of Systematic Reviews* **2013**, *6*.
1196 doi:10.1002/14651858.CD010609.
- 1197 93. Gonzalez de la Aleja, J.; Ramos, A.; Mato-Abad, V.; Martínez-Salio, A.; Hernández-Tamames, J.A.; Molina,
1198 J.A.; Hernández-Gallego, J.; Álvarez-Linera, J. Higher glutamate to glutamine ratios in occipital regions
1199 in women with migraine during the interictal state. *Headache: The Journal of Head and Face Pain* **2013**,
1200 *53*, 365–375.
- 1201 94. Chan, Y.M.; Pitchaimuthu, K.; Wu, Q.Z.; Carter, O.L.; Egan, G.F.; Badcock, D.R.; McKendrick, A.M. Relating
1202 excitatory and inhibitory neurochemicals to visual perception: A magnetic resonance study of occipital
1203 cortex between migraine events. *PLoS one* **2019**, *14*, e0208666.
- 1204 95. Siniatchkin, M.; Sendacki, M.; Moeller, F.; Wolff, S.; Jansen, O.; Siebner, H.; Stephani, U. Abnormal changes
1205 of synaptic excitability in migraine with aura. *Cerebral cortex* **2012**, *22*, 2207–2216.
- 1206 96. Albrecht, J.; Sidoryk-Wegrzynowicz, M.; Zielinska, M.; Aschner, M. Roles of glutamine in
1207 neurotransmission. *Neuron glia biology* **2010**, *6*, 263.
- 1208 97. Kanai, R.; Chaieb, L.; Antal, A.; Walsh, V.; Paulus, W. Frequency-dependent electrical stimulation of the
1209 visual cortex. *Current Biology* **2008**, *18*, 1839–1843.
- 1210 98. Smith, A.K.; Wade, A.R.; Penkman, K.E.; Baker, D.H. Dietary modulation of cortical excitation and
1211 inhibition. *Journal of Psychopharmacology* **2017**, *31*, 632–637.
- 1212 99. Peroutka, S.J. What turns on a migraine? A systematic review of migraine precipitating factors. *Current*
1213 *pain and headache reports* **2014**, *18*, 454.
- 1214 100. Baldacci, F.; Vedovello, M.; Ulivi, M.; Vergallo, A.; Poletti, M.; Borelli, P.; Nuti, A.; Bonuccelli, U. How
1215 aware are migraineurs of their triggers? *Headache: The Journal of Head and Face Pain* **2013**, *53*, 834–837.
- 1216 101. Neut, D.; Fily, A.; Cuvellier, J.C.; Vallée, L. The prevalence of triggers in paediatric migraine: a questionnaire
1217 study in 102 children and adolescents. *The journal of headache and pain* **2012**, *13*, 61–65.
- 1218 102. Spierings, E.L.; Ranke, A.H.; Honkoop, P.C. Precipitating and aggravating factors of migraine
1219 versus tension-type headache. *Headache: The journal of head and face pain* **2001**, *41*, 554–558.
1220 doi:10.1046/j.1526-4610.2001.041006554.x.
- 1221 103. Shepherd, A.J. Visual stimuli, light and lighting are common triggers of migraine and headache. *Journal of*
1222 *Light & Visual Environment* **2010**, *34*, 94–100.
- 1223 104. Wang, Y.J.; Chan, M.H.; Chen, L.; Wu, S.N.; Chen, H.H. Resveratrol attenuates cortical neuron activity:
1224 roles of large conductance calcium-activated potassium channels and voltage-gated sodium channels.
1225 *Journal of biomedical science* **2016**, *23*, 1–9.
- 1226 105. Peatfield, R.; Glover, V.; Littlewood, J.; Sandler, M.; Clifford Rose, F. The prevalence of diet-induced
1227 migraine. *Cephalalgia* **1984**, *4*, 179–183.
- 1228 106. Nowaczewska, M.; Wiciński, M.; Kaźmierczak, W.; Kaźmierczak, H. To Eat or Not to eat: A Review of the
1229 Relationship between Chocolate and Migraines. *Nutrients* **2020**, *12*, 608.

- 1230 107. Santiago-Rodríguez, E.; Estrada-Zaldívar, B.; Zaldívar-Uribe, E. Effects of dark chocolate intake on brain
1231 electrical oscillations in healthy people. *Foods* **2018**, *7*, 187.
- 1232 108. Marschollek, C.; Karimzadeh, F.; Jafarian, M.; Ahmadi, M.; Mohajeri, S.M.R.; Rahimi, S.; Speckmann, E.J.;
1233 Gorji, A. Effects of garlic extract on spreading depression: In vitro and in vivo investigations. *Nutritional*
1234 *neuroscience* **2017**, *20*, 127–134.
- 1235 109. Hougaard, A.; Amin, F.; Hauge, A.W.; Ashina, M.; Olesen, J. Provocation of migraine with aura using
1236 natural trigger factors. *Neurology* **2013**, *80*, 428–431.
- 1237 110. Bowyer, S.M.; Aurora, S.K.; Moran, J.E.; Tepley, N.; Welch, K. Magnetoencephalographic fields from
1238 patients with spontaneous and induced migraine aura. *Annals of Neurology: Official Journal of the American*
1239 *Neurological Association and the Child Neurology Society* **2001**, *50*, 582–587.
- 1240 111. Al-Shimmery, E.K. Precipitating and relieving factors of migraine headache in 200 iraqi kurdish patients.
1241 *Oman medical journal* **2010**, *25*, 212.
- 1242 112. Martin, P.R. How do trigger factors acquire the capacity to precipitate headaches? *Behaviour research and*
1243 *therapy* **2001**, *39*, 545–554.
- 1244 113. Herrmann, C.S. Human EEG responses to 1–100 Hz flicker: resonance phenomena in visual cortex and
1245 their potential correlation to cognitive phenomena. *Experimental brain research* **2001**, *137*, 346–353.
- 1246 114. Biglari, H.N.; Rezayi, A.; Biglari, H.N.; Alizadeh, M.; Ahmadabadi, F. Relationship between migraine and
1247 abnormal EEG findings in children. *Iranian journal of child neurology* **2012**, *6*, 21.
- 1248 115. Sand, T. Electroencephalography in migraine: a review with focus on quantitative electroencephalography
1249 and the migraine vs. epilepsy relationship. *Cephalalgia* **2003**, *23*, 5–11.
- 1250 116. Drake Jr, M.E.; Bois, C.D.; Huber, S.J.; Pakalnis, A.; Denio, L.S. EEG spectral analysis and time domain
1251 descriptors in headache. *Headache: The Journal of Head and Face Pain* **1988**, *28*, 201–203.
- 1252 117. Polich, J.; Ehlers, C.L.; Dalessio, D.J. Pattern-shift visual evoked responses and EEG in migraine. *Headache:*
1253 *The Journal of Head and Face Pain* **1986**, *26*, 451–456.
- 1254 118. Guidetti, V. Computerized EEG Topography in Childhood Headache. *Cephalalgia* **1987**, *9*.
1255 doi:10.1177/0333102489009S10104.
- 1256 119. Nyrke, T.; Kangasniemi, P.; Lang, H. Alpha rhythm in classical migraine (migraine with aura):
1257 abnormalities in the headache-free interval. *Cephalalgia* **1990**, *10*, 177–181.
- 1258 120. Jonkman, E.; Lelieveld, M. EEG computer analysis in patients with migraine. *Electroencephalography and*
1259 *clinical neurophysiology* **1981**, *52*, 652–655.
- 1260 121. Facchetti, D.; Marsile, C.; Faggi, L.; Donati, E.; Kokodoko, A.; Poloni, M. Cerebral mapping in subjects
1261 suffering from migraine with aura. *Cephalalgia* **1990**, *10*, 279–284.
- 1262 122. Bjørk, M.H.; Stovner, L.J.; Engstrøm, M.; Stjern, M.; Hagen, K.; Sand, T. Interictal quantitative EEG in
1263 migraine: a blinded controlled study. *The Journal of headache and pain* **2009**, *10*, 331.
- 1264 123. Sand, T.; Zhitniy, N.; White, L.R.; Stovner, L.J. Visual evoked potential latency, amplitude and habituation
1265 in migraine: a longitudinal study. *Clinical neurophysiology* **2008**, *119*, 1020–1027.
- 1266 124. Sand, T.; White, L.; Hagen, K.; Stovner, L. Visual evoked potential and spatial frequency in migraine: a
1267 longitudinal study. *Acta Neurologica Scandinavica* **2009**, *120*, 33–37.
- 1268 125. Shibata, K.; Osawa, M.; Iwata, M. Pattern reversal visual evoked potentials in migraine with aura and
1269 migraine aura without headache. *Cephalalgia* **1998**, *18*, 319–323.
- 1270 126. Evers, S.; Quibeldey, F.; Grotemeyer, K.H.; Suhr, B.; Husstedt, I. Dynamic changes of cognitive habituation
1271 and serotonin metabolism during the migraine interval. *Cephalalgia* **1999**, *19*, 485–491.
- 1272 127. Judit, A.; Sandor, P.; Schoenen, J. Habituation of visual and intensity dependence of auditory evoked cortical
1273 potentials tends to normalize just before and during the migraine attack. *Cephalalgia* **2000**, *20*, 714–719.
- 1274 128. Shahaf, G.; Kuperman, P.; Bloch, Y.; Yariv, S.; Granovsky, Y. Monitoring migraine cycle dynamics with an
1275 easy-to-use electrophysiological marker—a pilot study. *Sensors* **2018**, *18*, 3918.
- 1276 129. Dow, D.J.; Whitty, C. Electro-encephalographic changes in migraine review of 51 cases. *The Lancet* **1947**,
1277 *250*, 52–54.
- 1278 130. Malik, A.B.; Alptekin, B.; Bajwa, Z.H. Chapter 34 - Classification of Headache. In *Essentials of*
1279 *Pain Medicine and Regional Anesthesia (Second Edition)*, Second Edition ed.; Benzon, H.T.; Raja, S.N.;
1280 Molloy, R.E.; Liu, S.S.; Fishman, S.M., Eds.; Churchill Livingstone: Philadelphia, 2005; pp. 277–281.
1281 doi:https://doi.org/10.1016/B978-0-443-06651-1.50038-1.

- 1282 131. Ganji, S. Basilar artery migraine: EEG and evoked potential patterns during acute stage. *Headache: The*
1283 *Journal of Head and Face Pain* **1986**, *26*, 220–223.
- 1284 132. Spina, I.L.; Vignati, A.; Porazzi, D. Basilar artery migraine: Transcranial Doppler EEG and SPECT from the
1285 aura phase to the end. *Headache: The Journal of Head and Face Pain* **1997**, *37*, 43–47.
- 1286 133. Soriani, S.; Scarpa, P.; Faggioli, R.; Carlo, L.D.; Voghenzi, A. Uncommon EEG Pattern in an 8-Year-Old
1287 Boy With Recurrent Migraine Aura Without Headache. *Headache: The Journal of Head and Face Pain* **1993**,
1288 *33*, 509–511.
- 1289 134. Pisani, F.; Fusco, C. Ictal and interictal EEG findings in children with migraine. *The Journal of headache and*
1290 *pain* **2004**, *5*, 23.
- 1291 135. Ramelli, G.; Sturzenegger, M.; Donati, F.; Karbowski, K. EEG findings during basilar migraine attacks in
1292 children. *Electroencephalography and clinical neurophysiology* **1998**, *107*, 374–378.
- 1293 136. Sansone, M.; Marinelli, G.; Piccotti, E.; Severino, M.; Nobili, L. Cerebral blood flow in a case of typical aura
1294 without headache. *Journal of Neurology* **2019**, *266*, 2869–2871.
- 1295 137. Tan, H.; Suganthi, C.; Dhachayani, S.; Rizal, A.; Raymond, A. The electroencephalogram changes in
1296 migraineurs. *The Medical journal of Malaysia* **2007**, *62*, 56–58.
- 1297 138. Woods, R.P.; Iacoboni, M.; Mazziotta, J.C. Bilateral spreading cerebral hypoperfusion during spontaneous
1298 migraine headache. *New England Journal of Medicine* **1994**, *331*, 1689–1692.
- 1299 139. Lauritzen, M.; Olsen, T.S.; Lassen, N.A.; Paulson, O.B. Regulation of regional cerebral blood flow during
1300 and between migraine attacks. *Annals of Neurology: Official Journal of the American Neurological Association*
1301 *and the Child Neurology Society* **1983**, *14*, 569–572.
- 1302 140. Friberg, L.; Olesen, J.; Lassen, N.A.; Olsen, T.S.; Karle, A. Cerebral oxygen extraction, oxygen consumption,
1303 and regional cerebral blood flow during the aura phase of migraine. *Stroke* **1994**, *25*, 974–979.
- 1304 141. Arngrim, N.; Schytz, H.W.; Britze, J.; Amin, F.M.; Vestergaard, M.B.; Hougaard, A.; Wolfram, F.; de Koning,
1305 P.J.; Olsen, K.S.; Secher, N.H.; others. Migraine induced by hypoxia: an MRI spectroscopy and angiography
1306 study. *Brain* **2016**, *139*, 723–737.
- 1307 142. Blank Jr, W.; Kirshner, H. The kinetics of extracellular potassium changes during hypoxia and anoxia in
1308 the cat cerebral cortex. *Brain research* **1977**, *123*, 113–124.
- 1309 143. Lee, C.H.; Seo, M.W.; Shin, B.S.; Yang, T.H.; Shin, H.J.; Ryu, H.U. Intermittent theta slowings in contralateral
1310 side of weakness after sleep deprivation on spot EEG in sporadic hemiplegic migraine. *Journal of epilepsy*
1311 *research* **2016**, *6*, 102.
- 1312 144. Rey, V.; Aybek, S.; Maeder-Ingvar, M.; Rossetti, A.O. Positive occipital sharp transients of sleep (POSTS): a
1313 reappraisal. *Clinical neurophysiology* **2009**, *120*, 472–475.
- 1314 145. Speckman, E.; Elger, C.; Gorji, A. Neurophysiologic basis of EEG and DC potentials In: Schomer DL, Lopes
1315 da Silva FH, editors. Neidermeyer's electroencephalography, 2013.
- 1316 146. Caspers, H.; Speckmann, E.J. DC Shifts, EEG Waves and Neuronal Membrane Potentials in the Cat Cerebral
1317 Cortex during Seizure Activity. In *The Responsive Brain*; Elsevier, 1976; pp. 195–199.
- 1318 147. Áfra, J.; Mascia, A.; Phy, P.G.; De Noordhout, A.M.; Schoenen, J. Interictal cortical excitability in migraine:
1319 a study using transcranial magnetic stimulation of motor and visual cortices. *Annals of Neurology: Official*
1320 *Journal of the American Neurological Association and the Child Neurology Society* **1998**, *44*, 209–215.
- 1321 148. Brighina, F.; Piazza, A.; Daniele, O.; Fierro, B. Modulation of visual cortical excitability in migraine
1322 with aura: effects of 1 Hz repetitive transcranial magnetic stimulation. *Experimental brain research* **2002**,
1323 *145*, 177–181.
- 1324 149. Akben, S.B.; Subasi, A.; Tuncel, D. Analysis of EEG signals under flash stimulation for migraine and
1325 epileptic patients. *Journal of medical systems* **2011**, *35*, 437–443.
- 1326 150. Schoenen, J.; Jamart, B.; Delwaide, P. Cartographie electroencephalographique dans les migraines
1327 en periodes critique et intercritique. *Revue d'électroencéphalographie et de neurophysiologie clinique* **1987**,
1328 *17*, 289–299.
- 1329 151. Hall, S.D.; Barnes, G.R.; Hillebrand, A.; Furlong, P.L.; Singh, K.D.; Holliday, I.E. Spatio-temporal imaging
1330 of cortical desynchronization in migraine visual aura: A magnetoencephalography case study. *Headache:*
1331 *The Journal of Head and Face Pain* **2004**, *44*, 204–208.
- 1332 152. Seri, S.; Cerquiglini, A.; Guidetti, V. Computerized EEG topography in childhood migraine between and
1333 during attacks. *Cephalalgia* **1993**, *13*, 53–56.

- 1334 153. daSilva Morgan, K.; Elder, G.J.; Collerton, D.; Taylor, J.P.; others. The utility and application of
1335 electrophysiological methods in the study of visual hallucinations. *Clinical Neurophysiology* **2018**,
1336 *129*, 2361–2371.
- 1337 154. Klimesch, W.; Sauseng, P.; Hanslmayr, S. EEG alpha oscillations: The inhibition–timing hypothesis.
1338 *Brain Research Reviews* **2007**, *53*, 63–88. doi:https://doi.org/10.1016/j.brainresrev.2006.06.003.
- 1339 155. Dugué, L.; Marque, P.; VanRullen, R. The phase of ongoing oscillations mediates the causal relation
1340 between brain excitation and visual perception. *Journal of neuroscience* **2011**, *31*, 11889–11893.
- 1341 156. Jensen, O.; Gips, B.; Bergmann, T.O.; Bonnefond, M. Temporal coding organized by coupled alpha and
1342 gamma oscillations prioritize visual processing. *Trends in neurosciences* **2014**, *37*, 357–369.
- 1343 157. Lőrincz, M.L.; Kékesi, K.A.; Juhász, G.; Crunelli, V.; Hughes, S.W. Temporal framing of thalamic relay-mode
1344 firing by phasic inhibition during the alpha rhythm. *Neuron* **2009**, *63*, 683–696.
- 1345 158. Baumgarten, T.J.; Neugebauer, J.; Oeltzschner, G.; Füllenbach, N.D.; Kircheis, G.; Häussinger, D.; Lange,
1346 J.; Wittsack, H.J.; Butz, M.; Schnitzler, A. Connecting occipital alpha band peak frequency, visual
1347 temporal resolution, and occipital GABA levels in healthy participants and hepatic encephalopathy
1348 patients. *NeuroImage: Clinical* **2018**, *20*, 347–356.
- 1349 159. Shevelev, I.; Kamenkovich, V.; Bark, E.; Verkhutov, V.; Sharaev, G.; Mikhailova, E. Visual illusions and
1350 travelling alpha waves produced by flicker at alpha frequency. *International Journal of Psychophysiology*
1351 **2000**, *39*, 9–20.
- 1352 160. Walter, W.G. *The living brain.*; WW Norton, 1953.
- 1353 161. WALTER, W.G. Colour illusions and aberrations during stimulation by flickering light. *Nature* **1956**,
1354 *177*, 710–710.
- 1355 162. Walter, V.; Walter, W. The central effects of rhythmic sensory stimulation. *Electroencephalography & Clinical*
1356 *Neurophysiology* **1949**.
- 1357 163. Crotogino, J.; Feindel, A.; Wilkinson, F. Perceived scintillation rate of migraine aura. *Headache: The Journal*
1358 *of Head and Face Pain* **2001**, *41*, 40–48.
- 1359 164. Mauro, F.; Raffone, A.; VanRullen, R. A bidirectional link between brain oscillations and geometric patterns.
1360 *Journal of Neuroscience* **2015**, *35*, 7921–7926.
- 1361 165. Pearson, J.; Chiou, R.; Rogers, S.; Wicken, M.; Heitmann, S.; Ermentrout, B. Sensory dynamics of visual
1362 hallucinations in the normal population. *Elife* **2016**, *5*, e17072.
- 1363 166. Gert van Dijk, J.; Haan, J.; Ferrari, M. Photoc stimulation and the diagnosis of migraine. *Headache Quarterly*
1364 **1992**, *3*, 387–387.
- 1365 167. Fogang, Y.; Gérard, P.; De Pasqua, V.; Pepin, J.L.; Ndiaye, M.; Magis, D.; Schoenen, J. Analysis and clinical
1366 correlates of 20 Hz photic driving on routine EEG in migraine. *Acta Neurologica Belgica* **2015**, *115*, 39–45.
- 1367 168. Shibata, K.; Yamane, K.; Otuka, K.; Iwata, M. Abnormal visual processing in migraine with aura: a study
1368 of steady-state visual evoked potentials. *Journal of the neurological sciences* **2008**, *271*, 119–126.
- 1369 169. Shibata, K.; Yamane, K.; Nishimura, Y.; Kondo, H.; Otuka, K. Spatial frequency differentially affects
1370 habituation in migraineurs: a steady-state visual-evoked potential study. *Documenta ophthalmologica* **2011**,
1371 *123*, 65.
- 1372 170. Shiina, T.; Takashima, R.; Pascual-Marqui, R.D.; Suzuki, K.; Watanabe, Y.; Hirata, K. Evaluation of
1373 electroencephalogram using exact low-resolution electromagnetic tomography during photic driving
1374 response in patients with migraine. *Neuropsychobiology* **2019**, *77*, 186–191.
- 1375 171. De Graaf, T.A.; Gross, J.; Paterson, G.; Rusch, T.; Sack, A.T.; Thut, G. Alpha-band rhythms in visual task
1376 performance: phase-locking by rhythmic sensory stimulation. *PloS one* **2013**, *8*, e60035.
- 1377 172. Keitel, C.; Quigley, C.; Ruhnau, P. Stimulus-driven brain oscillations in the alpha range: entrainment of
1378 intrinsic rhythms or frequency-following response? *Journal of Neuroscience* **2014**, *34*, 10137–10140.
- 1379 173. Gerster, M.; Berner, R.; Sawicki, J.; Zakharova, A.; Škoch, A.; Hlinka, J.; Lehnertz, K.; Schöll, E.
1380 FitzHugh–Nagumo oscillators on complex networks mimic epileptic-seizure-related synchronization
1381 phenomena? A3B2 show [editpick]?. *Chaos: An Interdisciplinary Journal of Nonlinear Science* **2020**,
1382 *30*, 123130.
- 1383 174. De Tommaso, M.; Stramaglia, S.; Marinazzo, D.; Trotta, G.; Pellicoro, M. Functional and effective
1384 connectivity in EEG alpha and beta bands during intermittent flash stimulation in migraine with and
1385 without aura. *Cephalalgia* **2013**, *33*, 938–947.

- 1386 175. Trotta, G.; Stramaglia, S.; Pellicoro, M.; Bellotti, R.; Marinazzo, D.; de Tommaso, M. Effective connectivity
1387 and cortical information flow under visual stimulation in migraine with aura. 5th IEEE International
1388 Workshop on Advances in Sensors and Interfaces IWASI. IEEE, 2013, pp. 228–232.
- 1389 176. de Tommaso, M.; Trotta, G.; Vecchio, E.; Ricci, K.; Siugzdaite, R.; Stramaglia, S. Brain networking analysis
1390 in migraine with and without aura. *The journal of headache and pain* **2017**, *18*, 98.
- 1391 177. de Tommaso, M.; Trotta, G.; Vecchio, E.; Ricci, K.; Van de Steen, F.; Montemurno, A.; Lorenzo, M.;
1392 Marinazzo, D.; Bellotti, R.; Stramaglia, S. Functional connectivity of EEG signals under laser stimulation in
1393 migraine. *Frontiers in human neuroscience* **2015**, *9*, 640.
- 1394 178. Ning, Y.; Zheng, R.; Li, K.; Zhang, Y.; Lyu, D.; Jia, H.; Ren, Y.; Zou, Y. The altered Granger causality
1395 connection among pain-related brain networks in migraine. *Medicine* **2018**, *97*.
- 1396 179. Martins, I.P.; Westerfield, M.; Lopes, M.; Maruta, C.; Gil-da Costa, R. Brain state monitoring for the future
1397 prediction of migraine attacks. *Cephalalgia* **2020**, *40*, 255–265.
- 1398 180. O’Hare, L.; Hibbard, P.B. Visual processing in migraine. *Cephalalgia* **2016**, *36*, 1057–1076.
- 1399 181. Shepherd, A.J. Increased visual after-effects following pattern adaptation in migraine: a lack of intracortical
1400 excitation? *Brain* **2001**, *124*, 2310–2318.
- 1401 182. Wagner, D.; Manahilov, V.; Loffler, G.; Gordon, G.E.; Dutton, G.N. Visual noise selectively degrades vision
1402 in migraine. *Investigative ophthalmology & visual science* **2010**, *51*, 2294–2299.
- 1403 183. Wagner, D.; Manahilov, V.; Gordon, G.E.; Loffler, G. Global shape processing deficits are amplified by
1404 temporal masking in migraine. *Investigative ophthalmology & visual science* **2013**, *54*, 1160–1168.
- 1405 184. Hammett, S.T.; Cook, E.; Hassan, O.; Hughes, C.A.; Rooslien, H.; Tizkar, R.; Larsson, J. GABA, noise and
1406 gain in human visual cortex. *Neuroscience letters* **2020**, *736*, 135294.
- 1407 185. Shepherd, A. Visual contrast processing in migraine. *Cephalalgia* **2000**, *20*, 865–880.
- 1408 186. Asher, J.M.; O’Hare, L.; Romei, V.; Hibbard, P.B. Typical lateral interactions, but increased contrast
1409 sensitivity, in migraine-with-aura. *Vision* **2018**, *2*, 7.
- 1410 187. Aldrich, A.; Hibbard, P.; Wilkins, A. Vision and hyper-responsiveness in migraine. *Vision* **2019**, *3*, 62.
- 1411 188. McKendrick, A.; Sampson, G. Low spatial frequency contrast sensitivity deficits in migraine are not visual
1412 pathway selective. *Cephalalgia* **2009**, *29*, 539–549.
- 1413 189. Yoon, J.H.; Maddock, R.J.; Rokem, A.; Silver, M.A.; Minzenberg, M.J.; Ragland, J.D.; Carter, C.S. GABA
1414 concentration is reduced in visual cortex in schizophrenia and correlates with orientation-specific surround
1415 suppression. *Journal of Neuroscience* **2010**, *30*, 3777–3781.
- 1416 190. Edden, R.A.; Muthukumaraswamy, S.D.; Freeman, T.C.; Singh, K.D. Orientation discrimination
1417 performance is predicted by GABA concentration and gamma oscillation frequency in human primary
1418 visual cortex. *Journal of Neuroscience* **2009**, *29*, 15721–15726.
- 1419 191. McKendrick, A.M.; Vingrys, A.J.; Badcock, D.R.; Heywood, J.T. Visual dysfunction between migraine
1420 events. *Investigative ophthalmology & visual science* **2001**, *42*, 626–633.
- 1421 192. Tibber, M.S.; Guedes, A.; Shepherd, A.J. Orientation discrimination and contrast detection thresholds in
1422 migraine for cardinal and oblique angles. *Investigative ophthalmology & visual science* **2006**, *47*, 5599–5604.
- 1423 193. Wilkinson, F.; Crotopino, J. Orientation discrimination thresholds in migraine: a measure of visual cortical
1424 inhibition. *Cephalalgia* **2000**, *20*, 57–66.
- 1425 194. Pitchaimuthu, K.; Wu, Q.z.; Carter, O.; Nguyen, B.N.; Ahn, S.; Egan, G.F.; McKendrick, A.M. Occipital
1426 GABA levels in older adults and their relationship to visual perceptual suppression. *Scientific Reports* **2017**,
1427 *7*, 1–11.
- 1428 195. Battista, J.; Badcock, D.R.; McKendrick, A.M. Migraine increases centre-surround suppression for drifting
1429 visual stimuli. *PloS one* **2011**, *6*, e18211.
- 1430 196. Yazdani, P.; Serrano-Pedraza, I.; Whittaker, R.G.; Trevelyan, A.; Read, J.C. Two common psychophysical
1431 measures of surround suppression reflect independent neuronal mechanisms. *Journal of vision* **2015**,
1432 *15*, 21–21.
- 1433 197. Schallmo, M.P.; Millin, R.; Kale, A.M.; Kolodny, T.; Edden, R.A.; Bernier, R.A.; Murray, S.O. Glutamatergic
1434 facilitation of neural responses in MT enhances motion perception in humans. *NeuroImage* **2019**,
1435 *184*, 925–931.
- 1436 198. Takeuchi, T.; Yoshimoto, S.; Shimada, Y.; Kochiyama, T.; Kondo, H.M. Individual differences in visual
1437 motion perception and neurotransmitter concentrations in the human brain. *Philosophical Transactions of the*
1438 *Royal Society B: Biological Sciences* **2017**, *372*, 20160111.

- 1439 199. Antal, A.; Temme, J.; Nitsche, M.; Varga, E.; Lang, N.; Paulus, W. Altered motion perception in migraineurs:
1440 evidence for interictal cortical hyperexcitability. *Cephalalgia* **2005**, *25*, 788–794.
- 1441 200. Tibber, M.S.; Kelly, M.G.; Jansari, A.; Dakin, S.C.; Shepherd, A.J. An inability to exclude visual noise in
1442 migraine. *Investigative ophthalmology & visual science* **2014**, *55*, 2539–2546.
- 1443 201. Shepherd, A.J.; Wyatt, G.; Tibber, M.S. Visual metacontrast masking in migraine. *Cephalalgia* **2011**,
1444 *31*, 346–356.
- 1445 202. Drummond, P.D.; Anderson, M. Visual field loss after attacks of migraine with aura. *Cephalalgia* **1992**,
1446 *12*, 349–352.
- 1447 203. McKendrick, A.M.; Badcock, D.R. Decreased visual field sensitivity measured 1 day, then 1 week, after
1448 migraine. *Investigative ophthalmology & visual science* **2004**, *45*, 1061–1070.
- 1449 204. Nguyen, B.N.; Vingrys, A.J.; McKendrick, A.M. The effect of duration post-migraine on visual
1450 electrophysiology and visual field performance in people with migraine. *Cephalalgia* **2014**, *34*, 42–57.
- 1451 205. McKendrick, A.M.; Chan, Y.M.; Vingrys, A.J.; Turpin, A.; Badcock, D.R. Daily vision testing can expose the
1452 prodromal phase of migraine. *Cephalalgia* **2018**, *38*, 1575–1584.
- 1453 206. Luedtke, K.; Schulte, L.H.; May, A. Visual processing in migraineurs depends on the migraine cycle. *Annals*
1454 *of neurology* **2019**, *85*, 280–283.
- 1455 207. Schulte, L.H.; May, A. The migraine generator revisited: continuous scanning of the migraine cycle over 30
1456 days and three spontaneous attacks. *Brain* **2016**, *139*, 1987–1993.
- 1457 208. Shepherd, A.J. Tracking the migraine cycle using visual tasks. *Vision* **2020**, *4*, 23.
- 1458 209. Ergenoglu, T.; Demiralp, T.; Bayraktaroglu, Z.; Ergen, M.; Beydagi, H.; Uresin, Y. Alpha rhythm of the EEG
1459 modulates visual detection performance in humans. *Cognitive brain research* **2004**, *20*, 376–383.
- 1460 210. Hanslmayr, S.; Klimesch, W.; Sauseng, P.; Gruber, W.; Doppelmayr, M.; Freunberger, R.; Pecherstorfer, T.
1461 Visual discrimination performance is related to decreased alpha amplitude but increased phase locking.
1462 *Neuroscience letters* **2005**, *375*, 64–68.
- 1463 211. Hanslmayr, S.; Aslan, A.; Staudigl, T.; Klimesch, W.; Herrmann, C.S.; Bäuml, K.H. Prestimulus oscillations
1464 predict visual perception performance between and within subjects. *Neuroimage* **2007**, *37*, 1465–1473.
- 1465 212. Shibata, K.; Osawa, M.; Iwata, M. Pattern reversal visual evoked potentials in classic and common migraine.
1466 *Journal of the neurological sciences* **1997**, *145*, 177–181.
- 1467 213. Shibata, K.; Yamane, K.; Iwata, M.; Ohkawa, S. Evaluating the effects of spatial frequency on migraines by
1468 using pattern-reversal visual evoked potentials. *Clinical Neurophysiology* **2005**, *116*, 2220–2227.
- 1469 214. O'Hare, L.; Menchinelli, F.; Durrant, S.J. Resting-state alpha-band oscillations in migraine. *Perception* **2018**,
1470 *47*, 379–396.
- 1471 215. Cao, Z. Developing a migraine attack prediction system using resting-state EEG. PhD thesis, University of
1472 Technology, Sydney, 2017.
- 1473 216. Borgdorff, P. Arguments against the role of cortical spreading depression in migraine. *Neurological research*
1474 **2018**, *40*, 173–181.
- 1475 217. Bolay, H.; Vuralli, D.; Goadsby, P.J. Aura and Head pain: relationship and gaps in the translational models.
1476 *The journal of headache and pain* **2019**, *20*, 1–15.
- 1477 218. Dreier, J.P. The role of spreading depression, spreading depolarization and spreading ischemia in
1478 neurological disease. *Nature medicine* **2011**, *17*, 439–447.
- 1479 219. Kroos, J.M.; Marinelli, I.; Diez, I.; Cortes, J.M.; Stramaglia, S.; Gerardo-Giorda, L. Patient-specific
1480 computational modeling of cortical spreading depression via diffusion tensor imaging. *International*
1481 *journal for numerical methods in biomedical engineering* **2017**, *33*, e2874.
- 1482 220. Kroos, J.M.; de Tommaso, M.; Stramaglia, S.; Vecchio, E.; Burdi, N.; Gerardo-Giorda, L. Clinical correlates
1483 of mathematical modeling of cortical spreading depression: Single-cases study. *Brain and behavior* **2019**,
1484 *9*, e01387.
- 1485 221. Borsook, D.; Maleki, N.; Becerra, L.; McEwen, B. Understanding migraine through the lens of maladaptive
1486 stress responses: a model disease of allostatic load. *Neuron* **2012**, *73*, 219–234.
- 1487 222. Bigal, M.E.; Lipton, R.B. Concepts and mechanisms of migraine chronification. *Headache: The Journal of*
1488 *Head and Face Pain* **2008**, *48*, 7–15.
- 1489 223. Kunkel, R.S. Migraine aura without headache: benign, but a diagnosis of exclusion. *Cleveland Clinic journal*
1490 *of medicine* **2005**, *72*, 529.
- 1491 224. Olesen, J. International classification of headache disorders. *The Lancet Neurology* **2018**, *17*, 396–397.

- 1492 225. Chronicle, E.; Mulleners, W. Might migraine damage the brain? *Cephalalgia* **1994**, *14*, 415–418.
- 1493 226. Khalil, N.M.; Legg, N.J.; Anderson, D.J. Long term decline of P100 amplitude in migraine with aura.
1494 *Journal of Neurology, Neurosurgery & Psychiatry* **2000**, *69*, 507–511.
- 1495 227. Rocca, M.A.; Ceccarelli, A.; Falini, A.; Colombo, B.; Tortorella, P.; Bernasconi, L.; Comi, G.; Scotti, G.; Filippi,
1496 M. Brain gray matter changes in migraine patients with T2-visible lesions: a 3-T MRI study. *Stroke* **2006**,
1497 *37*, 1765–1770.
- 1498 228. Kurth, T.; Diener, H.C. Current views of the risk of stroke for migraine with and migraine without aura.
1499 *Current pain and headache reports* **2006**, *10*, 214–220.
- 1500 229. Hartings, J.A.; Shuttleworth, C.W.; Kirov, S.A.; Ayata, C.; Hinzman, J.M.; Foreman, B.; Andrew, R.D.;
1501 Boutelle, M.G.; Brennan, K.; Carlson, A.P.; others. The continuum of spreading depolarizations in acute
1502 cortical lesion development: examining Leao's legacy. *Journal of Cerebral Blood Flow & Metabolism* **2017**,
1503 *37*, 1571–1594.
- 1504 230. Orr, S.L.; Kabbouche, M.A.; O'Brien, H.L.; Kacperski, J.; Powers, S.W.; Hershey, A.D. Paediatric migraine:
1505 evidence-based management and future directions. *Nature Reviews Neurology* **2018**, *14*, 515–527.
- 1506 231. Merikangas, K.R. Contributions of epidemiology to our understanding of migraine. *Headache: The Journal*
1507 *of Head and Face Pain* **2013**, *53*, 230–246.
- 1508 232. Balestri, M.; Papetti, L.; Maiorani, D.; Capuano, A.; Tarantino, S.; Battan, B.; Vigevano, F.; Valeriani,
1509 M. Features of aura in paediatric migraine diagnosed using the ICHD 3 beta criteria. *Cephalalgia* **2018**,
1510 *38*, 1742–1747.
- 1511 233. Victor, T.; Hu, X.; Campbell, J.; Buse, D.; Lipton, R. Migraine prevalence by age and sex in the United
1512 States: a life-span study. *Cephalalgia* **2010**, *30*, 1065–1072.
- 1513 234. Stewart, W.; Wood, C.; Reed, M.; Roy, J.; Lipton, R. Cumulative lifetime migraine incidence in women and
1514 men. *Cephalalgia* **2008**, *28*, 1170–1178.
- 1515 235. MacGregor, E.A. Migraine, menopause and hormone replacement therapy. *Post reproductive health* **2018**,
1516 *24*, 11–18.
- 1517 236. Stewart, W.F.; Lipton, R.; Chee, E.; Sawyer, J.; Silberstein, S. Menstrual cycle and headache in a population
1518 sample of migraineurs. *Neurology* **2000**, *55*, 1517–1523.
- 1519 237. Ripa, P.; Ornello, R.; Degan, D.; Tiseo, C.; Stewart, J.; Pistoia, F.; Carolei, A.; Sacco, S. Migraine in
1520 menopausal women: a systematic review. *International journal of women's health* **2015**, *7*, 773.
- 1521 238. MacGregor, E.A. Oestrogen and attacks of migraine with and without aura. *The Lancet Neurology* **2004**,
1522 *3*, 354–361.
- 1523 239. Mattsson, P. Hormonal factors in migraine: A population-based study of women aged 40 to 74 years.
1524 *Headache: The Journal of Head and Face Pain* **2003**, *43*, 27–35.
- 1525 240. Kopell, B.S.; Lunde, D.T.; Clayton, R.B.; Moos, R.H. Variations in some measures of arousal during the
1526 menstrual cycle. *Journal of Nervous and Mental Disease* **1969**.
- 1527 241. Parlee, M.B. Menstrual rhythm in sensory processes: A review of fluctuations in vision, olfaction, audition,
1528 taste, and touch. *Psychological Bulletin* **1983**, *93*, 539.
- 1529 242. DeMarchi, G.; Tong, J. Menstrual, diurnal, and activation effects on the resolution of temporally paired
1530 flashes. *Psychophysiology* **1972**, *9*, 362–367.
- 1531 243. DIAMOND, M.; DIAMOND, A.L.; Mast, M. Visual sensitivity and sexual arousal levels during the
1532 menstrual cycle. *The Journal of nervous and mental disease* **1972**, *155*, 170–176.
- 1533 244. Ward, M.M.; Stone, S.C.; Sandman, C.A. Visual perception in women during the menstrual cycle. *Physiology*
1534 *& behavior* **1978**, *20*, 239–243.
- 1535 245. Barris, M.; Dawson, W.; Theiss, C. The visual sensitivity of women during the menstrual cycle. *Documenta*
1536 *Ophthalmologica* **1980**, *49*, 293–301.
- 1537 246. Scher, D.; Pionk, M.; Purcell, D.G. Visual sensitivity fluctuations during the menstrual cycle under dark
1538 and light adaptation. *Bulletin of the Psychonomic Society* **1981**, *18*, 159–160.
- 1539 247. Johnson, N.; Petersik, J.T. Preliminary findings suggesting cyclic changes in visual contrast sensitivity
1540 during the menstrual cycle. *Perceptual and motor skills* **1987**, *64*, 587–594.
- 1541 248. Webb, A.L.; Hibbard, P.B.; O'Gorman, R. Natural variation in female reproductive hormones does not
1542 affect contrast sensitivity. *Royal Society open science* **2018**, *5*, 171566.
- 1543 249. Deza, L.; Eidelberg, E. Development of cortical electrical activity in the rat. *Experimental neurology* **1967**,
1544 *17*, 425–438.

1545 © 2021 by the authors. Submitted to *Vision* for possible open access publication under the terms and conditions
1546 of the Creative Commons Attribution (CC BY) license (<http://creativecommons.org/licenses/by/4.0/>).